New femoral remains of *Nacholapithecus kerioi*: implications for intraspecific variation and Miocene hominoid evolution

Abstract

The middle Miocene stem kenyapithecine, *Nacholapithecus kerioi* (16–15 Ma; Nachola, Kenya), is represented by a large number of isolated fossil remains and one of the most complete skeletons in the hominoid fossil record (KNM-BG 35250). Multiple fieldwork seasons performed by Japanese-Kenyan teams during the last part of the 20th century resulted in the discovery of a large sample of *Nacholapithecus* fossils. Here, we describe new femoral remains of *Nacholapithecus*. In well-preserved specimens, we evaluate sex differences and within-species variation using both qualitative and quantitative traits. We use these data to determine whether these specimens are morphologically similar to the species holotype KNM-BG 35250 (which shows some plastic deformation), and to compare *Nacholapithecus* with other Miocene hominoids and extant anthropoids to evaluate the distinctiveness of its femur. The new fossil evidence reaffirms previously reported descriptions of some distal femoral traits, namely the morphology of the patellar groove. However, results also show that relative femoral head size in *Nacholapithecus* is smaller, relative neck length is longer, and neck-shaft angle is lower than previously reported for KNM-BG 35250. These traits have a strong functional signal related to the hip joint kinematics, suggesting that the morphology of the proximal femur in *Nacholapithecus* might be functionally related to quadrupedal-like behaviors instead of more derived antipronograde locomotor modes. Results further demonstrate that other African Miocene apes (with the exception of *Turkanapithecus kalakolensis*) generally fall within the *Nacholapithecus* range of variation, whose overall femoral shape resembles that of *Ekembo* spp. and *Equatorius*

africanus. Our results accord with the previously inferred locomotor repertoire of *Nacholapithecus*, indicating a combination of generalized arboreal quadrupedalism combined with other antipronograde behaviors (e.g., vertical climbing).

Keywords: Miocene hominoids; Femur; Functional morphology; Positional behavior

1. Introduction

Nacholapithecus kerioi is an extinct hominoid (subfamily Kenyapithecinae, tribe Equatorini) known from the middle Miocene of Kenya (Ishida et al., 1999). Fossil remains belonging to this taxon were found within the Aka Aitheputh Formation (Samburu County, Kenya) in Nachola (Fig. 1), that have been dated at 16–15 Ma (Nakatsukasa et al., 1998; Sawada et al., 1998; Ishida et al., 1999; Nakatsukasa and Kunimatsu, 2009). Originally, the material found in this area was attributed to the genus *Kenyapithecus*, either as *Kenyapithecus* sp. or *Kenyapithecus* cf. *africanus*, by several authors (Ishida et al., 1984; Rose et al., 1996; Nakatsukasa et al., 1998). Later, Ishida and colleagues (1999) erected the new genus and species *Nacholapithecus kerioi* with sufficient evidence to differentiate this taxon from other fossil hominoids.

Initial studies of the postcranial anatomy of *Nacholapithecus* were based on two dozen isolated fossil remains collected in the 1980s (most described by Rose et al., 1996) and a partial skeleton (holotype, KNM-BG 35250), as well as some other specimens recovered in the 1990s (Rose et al., 1996; Nakatsukasa et al., 1998, 2003a, b, 2007a, b, 2012; Ishida et al., 2004; Senut et al., 2004; Nakatsukasa and Kunimatsu, 2009; Pina et al., 2018; Takano et al., 2018, 2020). The basic body plan of *Nacholapithecus* (e.g., narrow thorax and long lumbar spine) is similar to that of *Ekembo* spp., which are considered arboreal quadrupeds engaging in cautious climbing

and clambering (Ward, 2015). However, *Nacholapithecus* also shows more derived features, such as longer pedal digits, an anterior projection of the ulnar coronoid process, a more mobile humeroradial joint, and a higher femoral neck-shaft angle (Nakatsukasa et al., 1998, 2004, 2007a; Ishida et al., 2004; Takano et al., 2018, 2020). These derived features provide insights into the positional behavior of *Nacholapithecus*, which includes some of the earliest evidence of forelimb-dominated behaviors with the enhancement of vertical climbing capabilities. No specific adaptations for below-branch suspension have been identified, although this positional behavior cannot be completely discarded on the basis of the current evidence (Nakatsukasa and Kunimatsu, 2009; Takano et al., 2018, 2020).

Fortunately, the Nachola area is very rich in fossil remains, and excavations since 2000 have unearthed a large number of fossils attributed to *Nacholapithecus*, resulting in an impressive and unusual collection in comparison with those of other Miocene hominoid taxa. The *Nacholapithecus* fossil collection comprises several fossils representing the same anatomical element, providing an opportunity to assess intraspecific morphological variation, which is rare within the hominoid fossil record. During the past decade, a number of studies have published on these specimens (Kikuchi et al., 2012, 2015, 2016, 2018; Ogihara et al., 2016; Takano et al., 2020).

An initial body mass of 20–23 kg was estimated for *Nacholapithecus* males (Rose et al., 1996; Ishida et al., 2004; Nakatsukasa and Kunimatsu, 2009). Recently, Kikuchi et al. (2018) estimated body mass from femoral head dimensions obtained from 12 fragments (see Kikuchi et al., 2018: Table 2). These authors reported the presence of marked sexual dimorphism in *Nacholapithecus*' body mass, with males estimated at an average of two times the body mass of females (see also Ishida et al., 1991 for sexual dimorphism estimated from the canines). They assigned six femora of the sample to

males (larger) and six to females (smaller) based on their body mass results. Kikuchi et al. (2018) briefly described the femoral specimens, but their focus was on investigating sexual dimorphism. In addition, they were highly selective and did not use specimens with damaged femoral heads. Thus, femoral anatomical features and their functional implications have not been thoroughly addressed.

This study focuses on reporting and describing femoral remains attributed to *Nacholapithecus,* as well as investigating the range of intraspecific variation and sex differences in this taxon using a combination of qualitative and quantitative traits. We use these data to determine the extent to which the well-preserved *Nacholapithecus* femora are similar to those of the holotype (whose distorted nature has been reported elsewhere; e.g., Nakatsukasa et al., 2012). We further compare *Nacholapithecus* with other African and Eurasian Miocene hominoids and extant anthropoids. Collectively, these comparisons and analyses allow us to review the *Nacholapithecus* species diagnosis and morphology in detail, and to evaluate the distinctiveness of its femur. A well-defined femoral morphology diagnosis will contribute to a better understanding of the *Nacholapithecus* positional behavior and its role within the locomotor evolution of the Hominoidea.

2. Materials and methods

2.1. Samples

The femoral material from the Nachola fossil sites housed at the National Museums of Kenya (Nairobi) labeled as '*Nacholapithecus*', '*Kenyapithecus* sp.', and 'Hominoidea' was reviewed to evaluate its taxonomic diagnosis at the species level. A total of 28 femoral remains was available for *Nacholapithecus* (Table 1).

Owing to taphonomic damage (described in detail below), morphometric comparisons are limited and only possible for a reduced number of femoral fragments (see Table 1). When possible (exclusively in nondistorted, nondamaged specimens/regions), selected measurements were taken and then used to quantitatively compare *Nacholapithecus* with other African and Eurasian Miocene hominoids and a wide range of extant anthropoid primates, including platyrrhines, colobines, cercopithecines and hominoids (Fig. 2; Table 2). The Miocene hominoid sample (Fig. 3; taxonomy after Alba, 2012) includes: the afropithecid *Morotopithecus bishopi* (UMP MORII 94'80; MacLatchy et al., 2000); the proconsulids *Proconsul major* (combination of NAP IX 46'99, NAP IX B 64, NAP IX 65 P. 67 fragments; Gommery et al., 1998, 2002; Senut et al., 2000), *Turkanapithecus kalakolensis* (KNM-WK 16950I; Leakey et al., 1988), *Ekembo nyanzae* (KNM-MW 13142A and KNM-RU 5527; Harrison, 1982; Ward et al., 1993), the kenyapithecine *Equatorius africanus* (BMNH M.16331; BMNH M.16332-3 is used for qualitative comparisons only; Le Gros Clark and Leakey, 1951; McCrossin, 1994), and the dryopithecines *Dryopithecus fontani* (IPS 41724; Moyà-Solà et al., 2009; Pina et al., 2019) and *Hispanopithecus laietanus* (IPS 18800.29; Moyà-Solà and Köhler, 1996; Pina et al., 2012).

2.2. Measurements

Linear measurements of the proximal femur were taken to the nearest 0.1 mm using digital calipers (Fig. 2). Superoinferior heights of the femoral head (SIH) and femoral neck (SIN), and anteroposterior depth (APN) of the femoral neck were used to create an index of the relative size of the head: SIH/(ÖSIN*APN). Relative length of the femoral neck (relative NL) was estimated by dividing neck length by the total mediolateral width of the proximal end of the femur (TotW; relative NL = NL/TotW x

100). Neck-shaft angle (NSangle) was measured from photographs of femora in anterior view using Fiji version 2.0 (Schindelin et al., 2012). The SIH/(ÖSIN*APN) and the NSangle have been traditionally associated with range of hip excursion and joint mobility (the larger the relative size of the head and the NSangle, the greater the motion of the joint), whereas relative NL has been related to the actions of the gluteal muscles during locomotion (the longer the length, the greater the length of the moment arm of the muscles and bending forces supported; Fleagle and Meldrum, 1988; Ruff, 1988; Aiello and Dean, 1990; Lovejoy et al., 2002; Harmon, 2007).

2.3. Analyses

Descriptive statistics (sample sizes, means, standard deviations and ranges) were computed for the SIH/(ÖSIN*APN), relative NL, and NSangle in *Nacholapithecus* (Table 3; see also Table 1 for *Nacholapithecus* raw data and Supplementary Online Material [SOM] Table S1). Boxplots were used to visualize the range of within-species variation and to examine whether *Nacholapithecus* femoral morphology is distinctive from that of other African and European Miocene hominoids.

Quantitative statistical analyses were used to evaluate differences in SIH/(ÖSIN*APN), relative NL, and NSangle between male and female *Nacholapithecus*. Sex assignation follows the classification provided in Kikuchi et al. (2018; Table 1). In addition, comparisons among *Nacholapithecus* (sexes pooled) and extant anthropoids were also carried out to check for potential differences/similarities and defining locomotor affinities. The Shapiro-Wilk test was used to check for normality of the data. The null hypothesis of normally distributed data could not be rejected ($p > 0.05$) for relative NL and NSangle, but the ratio of SIH/(ÖSIN*APN) was not normally distributed ($p < 0.001$). Thus, to evaluate sexual dimorphism, mean

differences between male and female *Nacholapithecus* were tested using the two-tailed Student's t-test for NL and NSangle and the nonparametric Mann-Whitney U test for SIH/(ÖSIN*APN). Likewise, for comparisons of relative NL and NSangle between *Nacholapithecus* and extant anthropoids, the parametric analysis of variance (ANOVA) was used along with Student's t-tests for post-hoc comparisons between species, whereas the nonparametric Kruskal-Wallis and Mann-Whitney U tests were used for SIH/(ÖSIN*APN). The Bonferroni method was used to adjust for all multiple pairwise comparisons for every variable. All analyses were performed using the statistical package R v. 3.6 (R Core Group, 2017).

In addition to quantitative analyses, some morphological traits of the *Nacholapithecus* femora were also qualitatively compared with those of other Miocene hominoids (including African and Eurasian taxa) to better define the distinctiveness of the *Nacholapithecus* femoral shape.

3. Results

3.1. Morphological descriptions of femoral fragments attributed to Nacholapithecus

KNM-BG 17778 This small head fragment was mentioned previously in Ishida et al. (2004) and Nakatsukasa et al. (2012), but has not been formally described (Fig. 4A–B). It is a half-head fragment with a short portion (ca. 4 mm) of the neck. The position and shape of the fovea capitis suggest that it is an anterior hemi-sphere of a left femoral head. The epiphysis is fused. Its small size (SIH = 17.7 mm) indicates it probably belonged to a female.

KNM-BG 40844 A femoral head fragment, probably right (Fig. 4C–D). The fragment bears no epiphyseal line and this, together with its small size (ca. 14 mm

anteroposteriorly and ca. 13 mm proximodistally) suggests it belongs to an adult female. The fovea capitis is marked and placed in the distal half of the head.

KNM-BG 40964 A right proximal femur missing the neck, the head and part of the greater trochanter (Fig. 4E–F). The whole fragment is compressed anteroposteriorly. The lesser trochanter is damaged. Since juvenile specimens have been recovered in the same locality, the possibility that this femur belonged to an immature individual cannot be precluded. However, its size is consistent with that of adult female specimens.

KNM-BG 42757 A left proximal femoral fragment (Fig. 4G–J). Although it preserves all the gross anatomical structures, both the epiphysis and the shaft are severely crushed anteroposteriorly (see Fig. 4I). It likely belonged to a male specimen due to its large size (SIH = 24.8 mm). Despite its deformation, the femoral head shows a circular shape in anterior view and is positioned slightly below the most proximal peak of the greater trochanter. The notch between the greater trochanter and the head appears to be wide and deep.

KNM-BG 44953 This specimen includes a right and a left femur and some left hip bone fragments. The right femur (44953A) was described by Kikuchi et al. (2018) and the left counterpart (44953B) is described here (Fig. 4K–M). It is a left proximal femur fragment which lacks most proximal structures, i.e., the head, part of the neck, and the greater trochanter. This fragment is anteroposteriorly compressed. The lesser trochanter is slightly eroded and faces completely posteriorly. However, this morphology is probably a result of deformation (Fig. 4L).

KNM-BG 42779 A shaft fragment (ca. 91 mm) probably belonging to the most distal part of the diaphysis, without the distal epiphysis and any diagnostic trait available (Fig. 4N–P). It is crushed anteroposteriorly. Due to its large size, this femoral fragment likely belonged to a male.

KNM-BG 42738/42756C This proximal femur was recovered from site BG-I west (Fig. 5A–C), together with more than 30 other skeletal elements. Although this collection is still being sorted, most of the elements represent a single young adult male. We include this element in our report since it is associated with the KNM-BG 42732 distal femur fragment described below (Fig. 5F–I). A distal femoral shaft of the right counterpart is also described below (KNM-BG 42722; Fig. 5D, E).

KNM-BG 42738/42759C is a ca. 51 mm (proximodistally) long proximal portion of a left femur (Fig. 5A–C). Although Kikuchi et al. (2018) described it briefly, we believe this specimen deserves a more detailed description. It comprises two large pieces (the head/neck portion and the shaft/greater trochanter portion) that join perfectly. The tip of the greater trochanter is missing and the lesser trochanter is broken off from the base. The shaft is lost distally from the lesser trochanter base. The epiphyseal line of the head is completely fused and not visible. The head is almost intact, although the cortex is partially worn out on the anterior and posteroinferior aspects. The articular surface is wide anteriorly and posteriorly. In proximal view, the head is offset slightly anteriorly and weakly rotated posteriorly (Fig. 5A). The head and neck surfaces are more confluent in posterior view. However, the center of the head is almost on the central axis of the neck in proximal view. The fovea is lightly weathered and is located in the posteroinferior quarter of the articular surface. The cross-section of the neck is kidney-shaped. It is weakly concave anteriorly, convex posteriorly, and the inferior part is thicker than the superior part. The SIN = 16.5 mm and APN = 12.9 mm. The neck-shaft angle is 121º. The crista trochanterica is present on the neck (Fig. 5C). The posterior bar of the trochanteric fossa is well developed and runs to the base of the lesser trochanter. The posterior cortex of the shaft is badly damaged and displaced to the medullary cavity. The anterior cortex is also fractured, though to a lesser degree, and

displaced posteriorly, leaving a wide but shallow depression. The distal part of the great trochanter is protuberant laterally and slightly anteriorly (Fig. 5B, C). Distal and posterior to this protuberance is a small swelling along the distal break. This might be the most proximal part of the lower eminence of the gluteal tuberosity.

The shaft is ca. 26.5 mm wide (mediolaterally) and is markedly compressed anteroposteriorly at the distal break point. Despite this compression, the anterior cortex thickness (3.1 mm) is well preserved and not distorted (the posterior thickness is difficult to determine, since the cortex looks affected by the compression).

KNM-BG 42722 This specimen is a ca. 61 mm long distal shaft piece of a right femur belonging to the same individual as KNM-BG 42732 and KNM-BG 42738/42756C (Fig. 5). It measures >15 mm mediolaterally, 12.8 mm anteroposteriorly at the proximal break point, and 18.0 mm mediolaterally and 14.1 mm anteroposteriorly at the distal break point. Since the breaks are covered by matrix, cortex is not clearly visible. Surface features are not well developed (Fig. 5D–E). However, two blunt ridges are discernible, which help to identify the anatomical position of this fragment when it is compared with the distal femur of *Eq. africanus* (BNMH M 16332-3; SOM Fig. S1). One of the two ridges, which is sharper at the distal break point, is a continuation from the lateral supra-epicondylar line. The other more rounded ridge divides the shaft surface into the posterior and medial surfaces. The posterior surface is weakly convex mediolaterally. The medial, anterior and lateral surfaces are not clearly differentiated. The shaft cross-section is not symmetrical mediolaterally. Regarding the anteroposterior axis, the medial half is wider than the lateral one.

KNM-BG 42732 This distal femur is associated with the KNM-BG 42738/42756C proximal femur described by Kikuchi et al. (2018; see above). A distal femoral shaft of the right counterpart is also associated (KNM-BG 42722; see above).

This specimen is a ca. 68 mm long distal portion of a left femur (Fig. 5F–I). The epiphyseal line is visible all around where the epiphysis is preserved. It lacks the lateral condyle (and epicondyle). The medial condyle is intact. The width of the medial condyle is 15.6 mm and is visually comparable with that of the left femur (KNM-BG 35250J) of the holotype specimen (Ishida et al., 2004). Plastic deformation is minor, as is the distortion (slightly stronger on the lateral side of the shaft). The diaphyseal part suffered notably from erosion. At the level of the proximal break point, which is 45 mm apart from the epiphyseal line on the medial side, the original cortex remains only as a very small (ca. 4 mm wide) portion on the anteromedial surface (Fig. 5I). The break is 13.4 mm wide and 12.4 mm thick when the missing outer cortex is not taken into account. Assuming a thickness of the eroded outer layer of cortex of 1 mm (an estimate based on photogrammetry), the original dimension of the break would not exceed 16 mm mediolaterally and 15 mm anteroposteriorly. This shaft is rather thin, especially anteroposteriorly when compared with the distal femoral end, probably because it likely belonged to a young adult (note the diaphyseal line in Figure 5F, G). In the femur of *Eq. africanus* from Maboko (BNMH M 16332-3: Le Gros Clark and Leakey, 1951), the anteroposterior thickness at an equivalent point is ca. 18 mm (measurement taken from a museum-produced cast). The medial supra-epicondylar ridge is discernible although it is damaged by erosion. The lateral supra-epicondylar ridge (line) is less clear.

The distal end is approximately 32 mm anteroposteriorly (in anatomical position and measured at the midpoint of the proximodistal height of the medial condyle). The medial condyle is mediolaterally wide (ca. 15.6 mm) relative to the epiphysis (Fig. 5H).

The pit-like insertion for the collateral ligament is well marked on the medial epicondyle. The rim of the medial condyle is posteriorly and distally intact. However, both the anterior part of this rim and the continuing medial rim of the patellar surface is eroded. This damage probably reduced the articular surface width by ~1-2 mm. The lateral patellar surface rim is more eroded than the medial rim. However, the proximal border of the patellar surface is intact and the proximodistal height of both the medial and lateral surface rims are similar, resulting in a quadrilateral shape for the patellar surface. The medial two-thirds of the intercondylar notch is preserved. A round depression is observed on the lateral side of the medial condyle proximally, which is likely the attachment area of the posterior cruciate ligament. Otherwise, there are no remarkable features (e.g., buttresses: MacLatchy et al., 2000) observed.

The two specimens described below belong to previously described femoral remains from Nachola, whose former attributions (either anatomical or taxonomic) are revised here:

KNM-BG 15533 This fragment was formerly described as a partial femoral head by Rose et al. (1996). However, the articular surface shows an anteroposterior compression that is typical of the humeral head of this taxon (SOM Fig. S2A).

KNM-BG 15536 This is a femoral head fragment described by Rose et al. (1996) as belonging to *Nacholapithecus* (then *Kenyapithecus* sp.). However, the morphology around the fovea capitis (shallow and with an irregular articular surface depression adjacent to the fovea, with distinct bone absorptive pits) is not common among the femoral heads of this taxon. This femur fragment may, therefore, belong to another nonprimate mammal (SOM Fig. S2B).

3.2. Within-species variation in Nacholapithecus *and sex differences*

297 A summary of the main femoral traits described in this study and discussed in
298 the literature for *Nacholapithecus* can be found in SOM Table S2.
299 In quantitative terms, the range of variation is moderately narrow for
300 SIH/(ÖSIN*APN) and relative NL in *Nacholapithecus* (Fig. 6A, B), whereas it is greater
301 for the NSangle (Fig. 6C). Previous authors have noted that the KNM-BG 35250A
302 holotype femur could show some plastic deformation (Fig. 7H). In our results, KNM-
303 BG 35250A falls in an intermediate position within the *Nacholapithecus* range of
304 variation for the relative femoral head size (Fig. 6A). On the other hand, excepting
305 KNM-BG 40826 (whose NSangle value should be considered with caution given the
306 fragmentary nature of this specimen), all the remaining *Nacholapithecus* specimens
307 show NSangle values below KNM-BG 35250A (Fig. 6C). Our quantitative results do
308 not show a clear trend for KNM-BG 35250A within the whole *Nacholapithecus* femora
309 sample that allows us to clearly associate it to plastic deformation issues.
310 Qualitatively, the femoral remains of *Nacholapithecus* display a hemispherical
311 head in all cases and the articular surface is well differentiated from the neck. When
312 preserved, the fovea capitis is generally shallow and is placed on the distal half of the
313 articular surface. Previous authors highlighted the posterior location of the fovea capitis
314 (Nakatsukasa et al., 2012; Kikuchi et al., 2018), but we were unable to confirm the
315 location in these newly described specimens due to their fragmentary nature and/or the
316 poor preservation.
317 Nakatsukasa and colleagues (Nakatsukasa et al., 2012) suggested that the
318 anteversion of the femoral head in KNM-BG 35250A was due to deformation. The
319 newly described specimens shows slight anteversion; the displacement of the femoral
320 head compared to the neck is not marked (Fig. 5A). The configuration observed in the
321 larger femoral sample of *Nacholapithecus* might confirm the view of Nakatsukasa et al.

(2012). When the head and the greater trochanter are preserved, the head proximally projects slightly above the greater trochanter (Fig. 7A–C).

Due probably to distortion, the neck length could not be measured in KNM-BG 35250A; thus, quantitative comparisons are not possible with the holotype. However, qualitative comparisons suggest that the femoral neck of the *Nacholapithecus* holotype is shorter than that of other *Nacholapithecus* femoral remains (e.g., KNM-BG 38391A; Fig. 7A, H).

The presence of a lateral flare of the greater trochanter cannot be conclusively added to the morphological suite of features that characterize the *Nacholapithecus* femur. Among the sample, there are specimens with well-defined flaring (e.g., KNM-BG 44954A and KNM-BG 44953A; Fig. 7B), while others are characterized by minimal lateral expansion of this region (e.g., KNM-BG 38391A; Fig. 7A, see also 7C). As previously noted, it seems clear that when the lateral projection is evident, it occurs mainly at the distal part of the greater trochanter (Fig. 7B, F).

Previous authors (Ishida et al., 2004; Nakatsukasa et al., 2012; Kikuchi et al., 2018) have noted that the lesser trochanter is placed close to the femoral neck and that it faces posteromedially in *Nacholapithecus*. The best specimen in which to observe this trait is KNM-BG 17816, which perfectly preserves its original form (Fig. 7D, E; Rose et al., 1996). Although not complete, KNM-BG 40800F and KNM-BG 38391A also support this interpretation (Kikuchi et al., 2018; Fig. 7A). The close location of the lesser trochanter to the femoral neck and its posteromedial orientation can be considered diagnostic for *Nacholapithecus* (Fig. 7D, E).

Despite variation in size, there were no significant differences between males and females in any of the analyses performed: SIH/(ÖSIN*APN) ($U = 9$, $p = 0.90$); relative NL ($t = 2.26$, $df = 3$, $p = 0.12$,), or NSangle ($t = 0.62$, $df = 3$, $p = 0.58$; see also

Fig. 6). When quantitative comparisons were not possible, the strong sexual dimorphism in body size of *Nacholapithecus* permitted us to tentatively differentiate between male (large) and female (small) specimens on the basis of size (see male/female size differences in Fig. 7A, C; Kikuchi et al., 2018).

Due to the distorted nature of the distal femoral fragments attributed to *Nacholapithecus* (KNM-BG 35250B, KNM-BG 35250J, and KNM-BG 42779; KNM-BG 42732 is a young adult individual), only qualitative comparisons could be made for this region (Figs. 4, 5; SOM Table S2). As previously described for the *Nacholapithecus* holotype (KNM-BG 35250B and J; Fig. 7I), the patellar groove is square-shaped, wide, and shallow in the relatively well-preserved juvenile specimen (KNM-BG 42732; Fig. 5F). The intercondylar fossa seems wide in KNM-BG 42732, although it is not possible to verify this trait in the holotype specimen since the remains are highly compressed mediolaterally (KNM-BG 35250B) and anteroposteriorly (KNM-BG 35250J).

3.3. Comparisons with other Miocene hominoids

Previous studies have identified a series of femoral traits that distinguish *Nacholapithecus* from other Miocene hominoids (especially African taxa), mainly focusing on differences with *Ekembo* spp. (Nakatsukasa et al., 1998, 2012; Ishida et al., 2004). Our analysis of the new femora raises questions about the distinctiveness of *Nacholapithecus*, given the overall morphological similarities of the proximal end of the femur to that of *Ek. nyanzae* (e.g., KNM-MW 13142A and KNM-RU 5527; see below). The femoral morphology also shows some resemblance to that of *Eq. africanus* (BNMH M.16331) and *T. kalakolensis* (KNM-WK 16950I), and more clearly differs from *M.*

bishopi (UMP MORII 94’80), *P. major* (NAP IX 46’99) and the European dryopithecines in general terms (Fig. 3).

The femoral head relative size (SIH/(ÖSIN*APN)) range of *Nacholapithecus* only overlaps with *Ekembo* and *Equatorius* (Fig. 6A), with the index value of the holotype close to that of *Ekembo* (KNM-MW 13142A; Fig. 3D). *Morotopithecus* (UMP MORII 94’80; Fig. 3A) shows the lowest value (smallest relative femoral head) among fossils; whereas *Hispanopithecus* (IPS 18800.29; Fig. 3H) shows one of the highest values (largest relative femora head) for this index among extinct taxa, slightly below the KNM-BG 38391A *Nacholapithecus* specimen.

On the basis of the holotype (KNM-BG 35250A), which is probably plastically deformed (Fig. 7H), it has been suggested that femoral neck length of *Nacholapithecus* is relatively short when compared with *Ekembo* (Fig. 3D–E; Ishida et al., 2004; Nakatsukasa et al., 2012). Kikuchi et al. (2018) subsequently reinforced this suggestion with a larger sample of femoral remains (most of them also included in this study). When quantified, however, our results do not support the characterization of the *Nacholapithecus* femoral neck as relatively short compared with *Ekembo*. The range of variation in neck length is small in *Nacholapithecus* (Fig. 6B) and the *Ekembo* specimen KNM-MW 13142A falls within the range of *Nacholapithecus*; while KNM-RU 5527 falls below its lower limit but close to its range of variation. It can be noted that *Turkanapithecus* (KNM-WK 16950I; Fig. 3C) displays a relatively very long femoral neck compared with the Miocene fossil hominoids (as well as the extant anthropoids in our sample; Fig. 6B). The European dryopithecines display relatively shorter necks than *Nacholapithecus*, being *Hispanopithecus* the extinct taxon with the shortest relative neck length (Fig. 6B).

When all the available *Nacholapithecus* femora are considered, results show that the NSangle of this taxon is not especially high among the Miocene hominoid taxa (contra Nakatsukasa et al., 2012; Figs. 3 and 6C). All the specimens included in the latter group fall within the range of *Nacholapithecus* except *Turkanapithecus*, whose NSangle value is slightly higher than the uppermost limit of the *Nacholapithecus* range (Fig. 6C).

Most of the *Nacholapithecus* specimens display a lateral projection of the greater trochanter but it is not present in all the available femora (e.g., KNM-BG 44954A vs. KNM-BG 38291A; see above; Fig. 7A–C; Kikuchi et al., 2018). When it is present, the flare is evident at the base of the greater trochanter (Nakatsukasa et al., 2012; Kikuchi et al., 2018; Fig. 7B). This feature is also present in other Miocene hominoids (Fig. 3; Senut et al., 2000; Bacon, 2001) such as *Ekembo* (KNM-MW 13142A), *Turkanapithecus* (KNM-WK 16950I), *Proconsul* (reconstructed specimen from NAP IX), *Equatorius* (BNMH M.16331), and *Hispanopithecus* (IPS 18800.29). Only *Morotopithecus* (UMP MORII 94’80) and *Dryopithecus* (IPS 41724) show a very light lateral protrusion of the greater trochanter (Fig. 3A, G; MacLatchy et al., 2000; Nakatsukasa et al., 2012; Almécija et al., 2013; Pina et al., 2019). Due to the observed variation in the *Nacholapithecus* femora, neither the presence nor the absence of a greater trochanter lateral flare can be considered diagnostic for *Nacholapithecus*.

The posteromedial facing and relatively proximal position of the lesser trochanter in *Nacholapithecus* (Fig. 7D, E; e.g., Ishida et al., 2004) not only resembles that observed in *Ekembo* (KNM-MW 13142A; Ward et al., 1993, but see Nakatsukasa et al., 2012) and *Equatorius* (BMNH M16331), but also that described for *Morotopithecus* (UMP MORII 94’80; MacLatchy et al., 2000; Fig. 3A). However, the configuration of the lesser trochanter in *Turkanapithecus* (KNM-WK 16950I; Leakey et

al., 1988; Fig. 3C) clearly differs from that defined for *Nacholapithecus* by facing more posteriorly and by being positioned more distally M. Pina, pers. obs.). This is also the case for *Dryopithecus* (IPS 41724) and *Hispanopithecus* (IPS 18800.29), whose lesser trochanter is placed more distally and facing posteriorly or more medially, respectively (Pina 2016; Pina et al., 2019). In the case of *Proconsul* (reconstructed specimen from NAP IX; Fig. 3B), interpretations of the direction of the lesser trochanter conflict in the literature; Senut et al. (2000) suggested that the lesser trochanter faces posteriorly, whereas Gommery et al. (2002) advocated for a medial direction.

The newly available *Nacholapithecus* femora also confirm other traits formerly highlighted in the literature, e.g., the close proximity of the gluteal tuberosity to the greater trochanter (Fig. 7F, G). This trait differentiates *Nacholapithecus* from *Ekembo* (KNM-MW 13142A) since in *Ekembo*, the gluteal tuberosity is positioned more distally relative to the greater trochanter (Fig. 3D; Nakatsukasa et al., 2012). Although not well preserved, the position of the gluteal tuberosity in *Turkanapithecus* (KNM-WK 16950I) resembles that of *Ekembo* more than that of *Nacholapithecus* (Fig. 3C; Leakey et al., 1988). Only *Dryopithecus* (IPS 41724) displays a marked gluteal tuberosity among the dryopithecines of the sample (Pina et al., 2019). In this case, the gluteal tuberosity is positioned closer to the greater trochanter than in *Ekembo* and resembles the condition of *Nacholapithecus* (Fig. 3G).

The patellar groove shape of *Nacholapithecus* is quadrangular and shallow (Fig. 5; see also Fig. 7I; SOM Figure S3; SOM 3D Model S1), as in *Turkanapithecus* (KNM-WK 16950I; Fig. 3C; Leakey et al., 1988), *Morotopithecus* (UMP MORII 94’80; Fig. 3A; MacLatchy et al., 2000) and probably *Equatorius* (KNM-MB 24727; see McCrossin, 1994:fig. 38 and p. 162). Rose (1983) also noted that the patellar groove of *Ekembo* (e.g., KNM-RU 5527; Fig. 3E) is square-shaped and shallow. Nakatsukasa et

al. (2012:238, footnote Fig. 3) highlighted that “the patellar surface is trapezoidal with a more raised lateral rim” in KNM-RU 5527. This trait, together with the asymmetric width of the condyles in KNM-RU 5527, differentiates the *Ekembo* distal femur from that of *Nacholapithecus*. The condyles of KNM-RU 5527 (Nakatsukasa et al., 2012; Fig. 3E), KNM-WK 16950I (Leakey et al., 1988; Fig. 3C) and UMP MORII 94’80 (MacLatchy et al., 2000; Fig. 3A) display more asymmetric epicondyles than *Nacholapithecus*.

Finally, the asymmetrical cross-section of the distal shaft displayed by *Nacholapithecus* (medial half wider than the lateral one) resembles that of *Equatorius* (BNMH M 16332-3; McCrossin, 1994), although it is much thinner anteroposteriorly in the only available *Nacholapithecus* specimen (KNM-BG 42722), likely reflecting that it is an immature specimen.

3.4. Comparisons of Nacholapithecus *femora with those of extant anthropoids*

Nacholapithecus, together with African apes and platyrrhines, shows an intermediate position between cercopithecoids (smaller relative femoral heads) and Asian apes (larger femoral heads) for SIH/(ÖSIN*APN) (Fig. 6A), with some statistically significant differences (Table 4).

Nachalopithecus displays a long neck (NL) relative to the total mediolateral width of the proximal femur, not significantly different from that of platyrrhines (i.e., *Cebus apella* and atelids), orangutans, chimpanzees, and gorillas, but significantly different from colobines, cercopithecines, *Hylobates lar* and *Pan paniscus* (Table 4; Fig. 6B; SOM Table S3). We note that variation in relative NL is high in many of the extant anthropoids, particularly in cercopithecines and colobines (whose ranges overlap with those of the other taxa).

The neck-shaft angle (NSangle) of *Nacholapithecus* has been described as high, like that of gibbons or *Ateles* (Natasukasa et al., 2012). However, statistically, the *Nacholapithecus* NSangle differs significantly from both *H. lar* and the atelids, as well as *Pongo pygmaeus*, cercopithecines, colobines, *H. lar*, and *P. t. schweinfurthii* (Table 4; Fig. 6C; SOM Table S3).

Qualitatively, the gluteal tuberosity in the *Nacholapithecus* sample is well marked and situated close to the greater trochanter (Fig. 7F, G), as originally described for the holotype specimen (Nakatsukasa et al., 2012). Among extant hominoids, only gibbons are reported to show a marked gluteal tuberosity (Stern, 1972; Almécija et al., 2013). As in the case of *Nacholapithecus*, the gluteal tuberosity of gibbons is positioned close to the greater trochanter (Fig. 7K).

The distal end of the femur, KNM-BG 42732, which does not suffer from severe distortion, displays an ape-like distal epiphysis, relatively wider medio-laterally than thick antero-posteriorly (Fig. 5H). The patellar groove of *Nacholapithecus* is shallow and more similar in shape to lesser apes (*Hylobates*) than platyrrhyines (*Cebus*) (i.e., with an approximated quadrangular shape); the intercondylar fossa appears wider than in *Cebus* (SOM Figure S3; SOM 3D Models S1–S3).

4. Discussion

4.1 Within species variation in Nacholapithecus

Kikuchi and colleagues (2018; see also Ishida et al., 1991) reported a strong sexual dimorphism for *Nacholapithecus*. Nonetheless, differences in size among the *Nacholapithecus* remains might additionally suggest either 1) the presence of several anthropoid taxa or 2) the presence of two different species of *Nacholapithecus* in the Nachola area.

Apart from *Nacholapithecus*, other anthropoid taxa have been recovered in this region, namely *Nyanzapithecus* (Kunimatsu, 1992, 1997) and *Victoriapithecus* (Pickford et al., 1987). It is possible that the smaller femora ascribed to *Nacholapithecus* belong to *Nyanzapithecus*, which might be smaller in overall body size (Kunimatsu, 1992, 1997). Female *Nacholapithecus* and male *Nyanzapithecus* reportedly overlap in size based on dental dimensions (Kunimatsu, 1997). Thus, the smaller femora in our sample could represent male *Nyanzapithecus* remains (see also Kikuchi et al, 2018). Most of the femora included in the current study were collected in the BG-K locality, from which no *Nyanzapithecus* specimens have been formally identified thus far. From the extensive collection of primate fossils (~240 dental specimens) recovered from this locality, only a single fragment of maxilla has been preliminarily catalogued as a non-cercopithecoid small catarrhine (Y. Kunimatsu, unpublished data). This fragment could be potentially accommodated as a nyanzapithecine, but due to its poor preservation, its attribution remains provisional (a formal description has not been published yet). All of the other dental material of *Nyanzapithecus*, as well as material tentatively attributed to this genus as cf. *Nyanzapithecus* (29 specimens including published and unpublished ones), have been collected from another locality (BG-X) together with ca. 190 *Nacholapithecus* dental specimens (Y. Kunimatsu, unpublished data). Only two small femora (KNM-BG 17775 and KNM-BG 17778) were recovered from BG-X. Rose et al. (1996) described nine hominoid postcranial specimens collected from this locality. Other than these two femoral specimens, only one proximal phalanx (KNM-BG 15531: of unknown ray) is considerably smaller than pedal proximal phalanges (median rays) of male *Nacholapithecus* (Nakatsukasa et al., 2003b; see also Nakatsukasa et al., 2012). This proximal phalanx thus could belong to either a female *Nacholapithecus* or a male *Nyanzapithecus*, but it could also be a male *Nacholapithecus*

phalanx from a paramedian ray. Although further analysis would help to corroborate this hypothesis, given that *Nyanzapithecus* remains are rare in the area of Nachola, the possibility of currently assigning postcranial remains to non-*Nacholapithecus* taxa is very low (Ishida et al., 1984; Kunimatsu, 1997).

The species *Nacholapithecus kerioi* was erected on the basis of the KNM-BG 35250 skeleton by Ishida et al. (1999). In their article, these authors included other hominoid specimens discovered from Nachola to the species, although they did not specify catalogued numbers. Subsequent works have underpinned the homogeneity of the dental morphology (regardless the differences in size; e.g. Kunimatsu et al., 2004). The evident differences in size among our femoral sample between the smallest and the largest fragments are not reflected in the femoral morphology. *Nacholapithecus* body mass estimated by Kikuchi et al. (2018), based on the femoral diameter, ranges 8.7–10.8 kg for females and 17.3–25.8 kg for males (see their Table 2 BM1 estimates). The largest femur (KNM-BG 40800F) is associated with unpublished dental rows that do not show any diagnostic features to distinguish them from other specimens assigned to *Nacholapithecus* smaller specimens. The same applies for the second largest femur in the Kikuchi et al., (2018) dataset, the subadult KNM-BG 42738/42756C (Y. Kunimatsu, personal observation). These facts lead us to conclude that the femoral sample analyzed here are all attributable to a single species of *Nacholapithecus*.

In addition, the sample of femoral fragments attributed to *Nacholapithecus* allows us to shed light on the *Nacholapithecus* holotype and broaden the range of variation for comparison with other species. With the additional femoral remains, we have found that the holotype femora display some quantitative and qualitative differences from other *Nacholapithecus* specimens that might support the idea that the KNM-BG 35250 femora display rather severe deformation. KNM-BG 35250A has been

545 traditionally used to define the femoral diagnostic traits of *Nacholapithecus*, but our
546 results suggest that drawing morphofunctional inferences from the holotype of this
547 taxon would be ill advised (see below).
548
549 *4.2. Functional interpretations and positional behavior in* Nacholapithecus
550 The proximal end of the femur has been the focus of extensive study due to its
551 relation with the functionality of the hip and its potential association with different
552 locomotor modes in primates. Some of the most characteristic traits are found at the
553 head-neck complex. Ruff (1988) suggested that the increase in the femoral head
554 decoupled from that of the neck will result in the enhancement of the hip joint excursion
555 (see also Ward et al., 1993; Harmon, 2007; Hammond, 2014, among others). Likewise,
556 the higher the NSangle, the greater the mobility at the hip (Rose, 1983; Ward et al.,
557 1993; Lovejoy et al., 2002; Hammond, 2014). Thus, a large relative head and a high
558 NSangle enhance the capacity for hip abduction and external rotation of the leg. This
559 configuration also increases the angle of the hind limb related to the midline of the
560 body, which facilitates antipronograde behaviors such as vertical climbing (Stern and
561 Susman, 1981; Rose, 1983; Ward et al., 1993; Harrison, 1986; MacLatchy, 1996;
562 Hammond, 2014). By contrast, quadrupedal monkeys display relatively small heads,
563 short necks, and lower NSangles, which help to resist bending forces and movements of
564 the hind limb preferentially in the parasagittal plane (Fleagle, 1977; Rose, 1983; Fleagle
565 and Meldrum, 1988; Cooke and Tallman, 2012).
566 Overall, the enlarged sample of *Nacholapithecus* femora suggests that the femur
567 of this taxon is characterized by a relatively small head (SIH/[ÖSIN*APN]), a
568 moderately long neck relative to the total mediolateral width of the proximal end of the
569 femur, and an intermediate (or moderate) NSangle, compared with extant anthropoids

(Fig. 6). These analyses suggest that previous functional interpretations based on the femoral morphology of KNM-BG 35250, the *Nacholapithecus* holotype (Fig. 7H, I), should be revised. Although KNM-BG 35250A does not always represent an extreme condition in the *Nacholapithecus* sample for the variables analyzed here (Fig. 6), functional inferences based exclusively on this specimen must be considered cautiously due to its plastic deformation. Therefore, as the relative femoral head, neck length and neck-shaft angle have been related to hip mobility and the capability of abduction of the hind limb (Grand, 1968; Fleagle and Meldrum, 1988; Ruff, 1988; Aiello and Dean, 1990; Hammond; 2014), our results have important implications regarding locomotor inferences in *Nacholapithecus*, suggesting it might have a less mobile hip joint than previously proposed (e.g., Nakatsukasa et al., 2012).

Although quantitative analyses are not possible for the distal femur, the new evidence supports previous descriptions of *Nacholapithecus* as having an apparently shallow and square-shaped patellar groove (Fig. 5F and Fig. 6I; SOM 3D Model S1). The shape of the patellar groove is controversial since some authors have suggested a high degree of intraspecific variation in this feature in *Nacholapithecus*, with some individuals displaying a square shape and others a more trapezoidal outline of the groove (Rose et al., 1996). The shallow patellar groove of the *Nacholapithecus* distal femur accords with its previously described morphology of the patella, which exhibits some living ape-like affinities that probably foretell the specialized patellae of living great apes (Fig. 6L; Ward et al., 1995; Rose et al., 1996; Pina et al., 2014, 2020). *Nacholapithecus* also displays condyles that are subequal in size (Nakatsukasa et al., 2012), a trait typical of quadrupedal anthropoid monkeys in which loadings are equally distributed through the distal end of the femur (Rose, 1983; Georgiou et al., 2018; Sukhdeo et al., 2018).

The general evidence found for the *Nacholapithecus* femur suggests that only the patellofemoral articulation might show enhanced range of motion, since this taxon does not display the stabilization traits of this joint characteristic of quadrupedal monkeys (e.g., deep patellar groove at the femur and compartmentalized articular surface of the patella; Harrison, 1986; Ward et al., 1995; DeSilva et al. 2013; Pina et al., 2014, 2020). On the other hand, the hip joint might maintain more restricted movements in the parasagittal plane (also supported by distal femoral condyles and epicondyles similar in size). Although *Nacholapithecus* does not show the whole set of characteristics of the proximal femoral end traditionally related to abduction movements and external rotation of the hip (long neck, low greater trochanter related to the head, relatively large femoral head, among others; Lovejoy et al., 2002; Richmond and Jungers, 2008; Almécija et al., 2013), these movements cannot be completely ruled out from its positional repertoire. This morpho-evolutionary gradation at the femur is also found in *Morotopithecus* (limited hip abduction and less-restricted movements at the knee; MacLatchy et al., 2000) and departs from the femoral evidence observed in *Ekembo*, *Turkanapithecus* and *Equatorius*. The reviewed morphology of the *Nacholapithecus* femur presented in this work is completely compatible with the positional repertoire formerly proposed for this Miocene taxon, which probably combined generalized above-branch quadrupedalism with other antipronograde behaviors, such as vertical climbing (no clear evidence for suspension is found in its femur or elsewhere; Nakatsukasa et al., 2003b, 2012; Ishida et al., 2004; Nakatsukasa and Kunimatsu, 2009; Ogihara et al., 2016; Takano et al., 2018, 2020).

Results presented in this work suggest that the *Nacholapithecus* femur resembles those of *Ekembo*, *Turkanapithecus*, and *Equatorius*, showing a general primitive (stem hominoid-like) appearance. In contrast, *Nacholapithecus* differs from those femora

showing more derived (living hominoid-like) traits, such as *Morotopithecus* and *Proconsul* in Africa (MacLatchy et al., 2000; Senut et al., 2000; Gommery et al., 2002) and *Sivapithecus* in the late Miocene of Asia (Kelley, 2005; Madar et al., 2002). *Nacholapithecus* is also unlike the younger European hominids. Although also displaying quadrupedal affinities (Moyà-Solà et al., 2009; Pina et al., 2019), our results show that *Nacholapithecus* differs from *Dryopithecus* at the proximal end of the femur and clearly departs from those taxa with well-defined affinities for forelimb-dominated behaviors (i.e., *Hispanopithecus*, *Rudapithecus*, *Danuvius*, and *Oreopithecus*; Straus, 1963; Hürzeler, 1968; Harrison, 1986; Jungers, 1987; Begun 1992, 2013; Rose, 1993; Moyà-Solà and Köhler, 1996; Begun and Kordos, 2011; Begun et al., 2012; Pina et al., 2012; Böhme et al., 2019; Ward et al., 2019).

When the whole anatomy is taken into account, similarities between *Nacholapithecus* and *Ekembo* are less clear. Although the general body plan in these two taxa is similar (narrow and deep trunk; Ward et al., 1993; Nakatsukasa et al., 2007a), *Nacholapithecus* clearly departs from *Ekembo* regarding forelimb shape. The former displays a series of characteristics more related to the stabilization of the humeroantebrachial complex (e.g., anterior projection of the coronoid process of the ulna and globular humeral capitulum) and enhancement of the pronation-supination movements, as shown in the elbow of living apes (Nakatsukasa and Kunimatsu, 2009; Takano et al., 2018, 2020). As occurs in other Miocene taxa (not only in Africa, but also in Eurasia; see e.g., Pilbeam et al., 1980; Begun, 1992, 2015; Moyà-Solà and Köhler, 1996; Madar et al., 2002; Almécija et al., 2013; Ward, 2015; Böhme et al., 2019), the postcranial morphology of *Nacholapithecus* shows a unique combination of primitive and derived features; in general, a more derived forelimb, foot, and lumbar region, and a primitive hind limb compared with *Ekembo* (Ishida et al., 2004; Nakatsukasa and

Kunimatsu, 2009). These results are compatible with general inferences made for this taxon, but also for the rest of middle Miocene hominoids included in this work. Overall, these African primates potentially combined general arboreal quadrupedalism with other antipronograde behaviors (Rose, 1983; Nakatsukasa and Kunimatsu, 2009; Alba, 2012; Begun, 2012; Ward, 2015). In the case of *Nacholapithecus*, its forelimbs and feet were apparently more derived than its hind limbs and trunk. This fact could suggest the presence of selective pressures on the upper half of the body in Miocene African taxa, underpinning the development of forelimb-dominated behaviors such as vertical climbing and, more recently, below-branch suspension (Nakatsukasa and Kunimatsu, 2009). Although no specific traits for the latter locomotor mode or slow-cautious quadrupedalism have been identified in *Nacholapithecus* (Nakatsukasa and Kunimatsu, 2009; Takano et al., 2018, 2020), they cannot be entirely ruled out for the positional behavior repertoire of this taxon. Nonetheless, like the other middle Miocene hominoid taxa in this work, *Nacholapithecus* was likely adapted for an arboreal life, and some antipronograde behavior (e.g., vertical climbing, clambering, and/or cautious and eclectic climbing) could have been a component of its locomotor repertoire, though less than in middle and late Miocene Eurasian taxa (Nakatsukasa et al., 2003b; 2007a; 2012; Senut et al., 2000; Takano et al., 2018, 2020).

5. Conclusions

The study of a larger sample of femora assigned to *Nacholapithecus* allowed us to review the original description and species diagnostic femoral traits reported for KNM-BG 35250 (holotype). Our results show that the morphology of the better-preserved femora differs in some respects from that of the original description derived from the holotype (mainly at the femoral head and neck). These findings suggest that

previous interpretation of the femoral morphology of *Nacholapithecus* may have been influenced by the presence of some distortion and/or deformation in the holotype femora (see also Nakatsukasa et al., 2012). Consequently, in contrast with previous work, we found that the overall femoral morphology in *Nacholapithecus* is more similar to that of early and middle Miocene taxa (mainly *Ekembo* spp. and *Equatorius*) than previously thought. At the same time, the new femoral fragments provide qualitative support for some of the formerly proposed differences with other taxa, such as the relative position of the gluteal tuberosity.

In addition, our results highlight the more primitive (stem hominoid-like) appearance of the proximal femur in *Nacholapithecus*, in contrast to the more derived (extant hominoid-like) traits found in its forelimb, which clearly depart from those shown in *Ekembo* spp. Taking into account the whole evidence from *Nacholapithecus*, the mosaic condition of its postcranial skeleton fits well within the positional behavior scenario inferred for the early-middle Miocene of Africa (femoral morphology of *Nacholapithecus* clearly departs from those of the Eurasian Miocene hominoids). Most of the extinct hominoids found thus far would have a positional behavior repertoire that might include frequent use of general arboreal quadrupedalism combined with other ape-like antipronograde behaviors, such as vertical climbing. However, *Nacholapithecus* might have displayed certain enhancement of forelimb-dominated behaviors. Although further evolutionary studies are needed to corroborate this hypothesis, such a unique combination in the *Nacholapithecus* skeleton could be the origin of the more-derived behaviors found in younger Eurasian hominoids.

References

694 Aiello, L.C., Dean, C., 1990. The Hominoid Femur. In: Aiello, L.C., Dean, C. (Eds.),
695 An Introduction to Human Evolutionary Anatomy. Academic Press, London, pp.
696 457-482.
697 Alba, D.M., 2012. Fossil apes from the Vallès-Penedès Basin (NE Iberian Peninsula):
698 Phylogenetic, paleobiogeographic and paleobiological implications. Evol.
699 Anthropol. 21, 254-269.
700 Alba, D.M., Almécija, S., Casanovas-Vilar, I., Méndez, J.M., Moyà-Solà, S., 2012. A
701 partial skeleton of the fossil great ape *Hispanopithecus laietanus* from Can Feu
702 and the mosaic evolution of crown-hominoid positional behaviors. PLoS One 7,
703 e39617.
704 Almécija, S., Tallman, M., Alba, D.M., Pina, M., Moyà-Solà, S., Jungers, W.L., 2013.
705 The femur of *Orrorin tugenensis* exhibits morphometric affinities with both
706 Miocene apes and later hominins. Nat. Commun. 4, 2888.
707 Almécija, S., Tallman, M., Sallam, H.M., Fleagle, J.G., Hammond, A.S., Seiffert, E.R.,
708 2019. Early anthropoid femora reveal divergent adaptive trajectories in catarrhine
709 hind-limb evolution. Nat. Commun. 10, 4778.
710 Bacon, A.-M., 2001. La locomotion des Primates du Miocène d'Afrique et d'Europe.
711 Cahiers de paléoanthropologie. CNRS Éditions, Paris.
712 Begun, D.R., 1992. Phyletic Diversity and Locomotion in Primitive European
713 Hominids. Am J. Phys. Anthropol. 87, 311-340.
714 Begun, D.R., 2013. The Miocene Hominoid Radiations. In: Begun, D.R. (Ed.), A
715 companion to paleoanthropology. Blackwell Publishing, Chichester, UK, pp. 398-
716 416.

717 Begun, D.R., 2015. Fossil Record of Miocene Hominoids. In: Henke, W., Tattersall, I.
718 (Eds.), Handbook of Paleoanthropology. Springer, Berlin Heidelberg, pp. 1261-
719 1332.
720 Begun, D.R., Kivell, T.L., 2011. Knuckle-walking in *Sivapithecus*? The combined
721 effects of homology and homoplasy with possible implications for pongine
722 dispersals. J. Hum. Evol. 60, 158-170.
723 Begun, D.R., Kordos, L., 2011. New postcrania of *Rudapithecus hungaricus* from
724 Rudabánya (Hungary). Am J. Phys. Anthropol. S52, 86.
725 Begun, D.R., Nargolwalla, M.C., Kordos, L., 2012. European Miocene hominids and
726 the origin of the African ape and human clade. Evol. Anthropol. 21, 10-23.
727 Böhme, M., Spassov, N., Fuss, J., Tröscher, A., Deane, A.S., Prieto, J., Kirscher, U.,
728 Lechner, T., Begun, D.R., 2019. A new Miocene ape and locomotion in the
729 ancestor of great apes and humans. Nature 575, 489-493.
730 Cooke, S.B., Tallman, M., 2012. New endemic platyrrhine femur from Haiti:
731 Description and locomotor analysis. J. Hum. Evol. 63, 560-567.
732 DeSilva, J.M., Morgan, M.E., Barry, J.C., Pilbeam, D., 2010. A hominoid distal tibia
733 from the Miocene of Pakistan. J. Hum. Evol. 58, 147-154.
734 DeSilva, J.M., Holt, K.G., Churchill, S.E., Carlson, K.J., Walker, C.S., Zipfel, B.,
735 Berger, L.R., 2013. The Lower Limb and Mechanics of Walking in
736 *Australopithecus sediba*. Science 340.
737 Fleagle, J.G., 1977. Locomotor behavior and muscular anatomy of sympatric Malaysian
738 leaf-monkeys (*Presbytis obscura* and *Presbytis melalophos*). Am J. Phys.
739 Anthropol. 46, 297-307.

740 Fleagle, J.G., Meldrum, D.J., 1988. Locomotor behavior and skeletal morphology of
741 two sympatric pitheciine monkeys, *Pithecia pithecia* and *Chiropotes satanas*. Am
742 J. Primatol. 16, 227-249.
743 Georgiou, L., Kivell, T.L., Pahr, D.H., Skinner, M.M., 2018. Trabecular bone patterning
744 in the hominoid distal femur. PeerJ 6, e5156.
745 Gommery, D., Senut, B., Pickford, M., 1998. Nouveaux restes postcrâniens
746 d'Hominoidea du Miocène inférieur de Napak, Ouganda. Annales de
747 Paléontologie 84, 287-306.
748 Gommery, D., Senut, B., Pickford, M., Musiime, E., 2002. Les nouveaux restes du
749 squelette d'*Ugandapithecus major* (Miocène inférieur de Napak, Ouganda). Ann.
750 de Paléontol. 88, 167-186.
751 Grand, T.I., 1968. The functional anatomy of the lower limb of the howler monkey
752 (*Alouatta caraya*). Am J. Phys. Anthropol. 28, 163-181.
753 Hammond, A.S., 2014. *In vivo* baseline measurements of hip joint range of motion in
754 suspensory and nonsuspensory anthropoids. Am J. Phys. Anthropol. 153, 417-
755 434.
756 Hammond, A.S., Rook, L., Anaya, A.D., Cioppi, E., Costeur, L., Moyà-Solà, S.,
757 Almécija, S., 2020. Insights into the lower torso in late Miocene hominoid
758 *Oreopithecus bambolii*. Proc. Natl. Acad. Sci. USA 117, 278.
759 Harmon, E.H., 2007. The shape of the hominoid proximal femur: A geometric
760 morphometric analysis. J. Anat. 210, 170-185.
761 Harrison, T., 1982. Small-bodied apes from the Miocene of East Africa. Ph.D.
762 Dissertation, University College London.
763 Harrison, T., 1986. A reassessment of the phylogenetic relationships of *Oreopithecus*
764 *bambolii* Gervais. J. Hum. Evol. 15, 541-583.

765 Hürzeler, J., 1968. *Oreopithecus bambolii* Gervais. A preliminary report.
766 Verhandlungen Naturforchenden Gesellschaft Basel 69, 1-48.
767 Ishida, H., Pickford, M., Nakaya, H., Nakano, Y., 1984. Fossil anthropoids from
768 Nachola and Samburu Hills, Samburu District, Kenya. Afr. Study Monogr. Suppl.
769 Issue 2, 73-85.
770 Ishida, H., Mbua, E., Nakano, Y., Yasui, K., 1991. Sexual dimorphism in canine size of
771 *Kenyapithecus* from Nachola, Northern Kenya. In: Ehara, A., Kimura, T.,
772 Takenaka, O., Iwamoto, M. (Eds.), Primatology Today: Proceedings of the XIIIth
773 Congress of the International Primatological Society, Nagoya and Kyoto, 18-24
774 July 1990. Elsevier, Amsterdam, pp. 517-520.
775 Ishidal, H., Kunimatsu, Y., Nakatsukasa, M., Nakano, Y., 1999. New Hominoid Genus
776 from the Middle Miocene of Nachola, Kenya. Anthropol. Sci. 107, 189-191.
777 Ishida, H., Kuminatsu, Y., Takano, T., Nakano, Y., Nakatsukasa, M., 2004.
778 *Nacholapithecus* skeleton from the Middle Miocene of Kenya. J. Hum. Evol. 46,
779 69-103.
780 Jungers, W.L., 1987. Body size and morphometric affinities of the appendicular
781 skeleton in *Oreopithecus bambolii* (IGF 11778). J. Hum. Evol. 16, 445-456.
782 Kelley, J., 2005. Twenty-five years contemplating *Sivapithecus* taxonomy. In:
783 Lieberman, D.E., Smith, R.H., Kelley, J. (Eds.), Interpreting the Past: Essays on
784 Human, Primate, and Mammal Evolution in Honor of David Pilbeam. Brill
785 Academic Publishers, Boston, pp. 123-143.
786 Kikuchi, Y., Nakano, Y., Nakatsukasa, M., Kunimatsu, Y., Shimizu, D., Ogihara, N.,
787 Tsujikawa, H., Takano, T., Ishida, H., 2012. Functional morphology and anatomy
788 of cervical vertebrae in *Nacholapithecus kerioi*, a middle Miocene hominoid from
789 Kenya. J. Hum. Evol. 62, 677-695.

Kikuchi Y, Nakatsukasa M, Nakano Y, Kunimatsu Y, Shimizu D, Ogihara N, Tsujikawa H, Takano T, Ishida H. 2015. Morphology of the thoracolumbar spine of the middle Miocene hominoid *Nacholapithecus kerioi* from northern Kenya. J. Hum. Evol., 88, 25-42.

Kikuchi, Y., Nakatsukasa, M., Nakano, Y., Kunimatsu, Y., Shimizu, D., Ogihara, N., Tsujikawa, H., Takano, T., Ishida, H., 2016. Sacral vertebral remains of the Middle Miocene hominoid *Nacholapithecus kerioi* from northern Kenya. J. Hum. Evol. 94, 117-125.

Kikuchi, Y., Nakatsukasa, M., Tsujikawa, H., Nakano, Y., Kunimatsu, Y., Ogihara, N., Shimizu, D., Takano, T., Nakaya, H., Sawada, Y., Ishida, H., 2018. Sexual dimorphism of body size in an African fossil ape, *Nacholapithecus kerioi*. J. Hum. Evol. 123, 129-140.

Köhler, M., Alba, D.M., Moyà-Solà, S., MacLatchy, L., 2002. Taxonomic affinities of the Eppelsheim femur. Am J. Phys. Anthropol. 119, 297-304.

Kunimatsu, Y., 1992. New finds of a small anthropoid primate from Nachola, northern Kenya. Afr. Study Monogr. 13, 237-249.

Kunimatsu, Y., 1997. New Species of *Nyanzapithecus* from Nachola, Northern Kenya. Anthropol. Sci. 105, 117-141.

Kunimatsu, Y., Ishida, H., Nakatsukasa, M., Nakano, Y., Sawada, Y., Nakayama, K., 2004. Maxillae and associated gnathodental specimens of *Nacholapithecus kerioi*, a large-bodied hominoid frm Nachola, northern Kenya. J. Hum. Evol. 46, 365-400.

Leakey, R.E., Leakey, M.G., Walker, A.C., 1988. Morphology of *Turkanapithecus kalakolensis* from Kenya. Am J. Phys. Anthropol. 76, 277-288.

814 Le Gros Clark, W.E., Leakey, L.S.B., 1951. The Miocene Hominoidea of East Africa.
815 Foss. Mamm. Afr. 1, 1-117.
816 Lovejoy, C.O., Heiple, K.G., Burnstein, A.H., 1973. The gait of *Australopithecus*. Am
817 J. Phys. Anthropol. 38, 757-780.
818 Lovejoy, C.O., Meindl, R.S., Ohman, J.C., Heiple, K.G., White, T.D., 2002. The Maka
819 femur and its bearing on the antiquity of human walking: Applying contemporary
820 concepts of morphogenesis to the human fossil record. Am J. Phys. Anthropol.
821 119, 97-133.
822 MacLatchy, L.M., 1996. Another look at the australopithecine hip. J. Hum. Evol. 31,
823 455-476.
824 MacLatchy, L., Gebo, D., Kityo, R., Pilbeam, D., 2000. Postcranial functional
825 morphology of *Morotopithecus bishopi*, with implications for the evolution of
826 modern ape locomotion. J. Hum. Evol. 39, 159-183.
827 Madar, S.I., Rose, M.D., Kelley, J., MacLatchy, L., Pilbeam, D., 2002. New
828 *Sivapithecus* postcranial specimens from the Siwaliks of Pakistan. J. Hum. Evol.
829 42, 705-752.
830 McCrossin, M.L., 1994. The phylogenetic relationship, adaptations, and ecology of
831 *Kenyapithecus*. Ph.D. Dissertation, University of California.
832 McHenry, H.M., Corruccini, R.S., 1976. Fossil hominid femora and the evolution of
833 walking. Nature 259, 657-658.
834 McHenry, H.M., Corruccini, R.S., 1978. The femur in early human evolution. Am J.
835 Phys. Anthropol. 49, 473-488.
836 Morgan, M.l.E., Lewton, K.L., Kelley, J., Otárola-Castillo, E., Barry, J.C., Flynn, L.J.,
837 Pilbeam, D., 2015. A partial hominoid innominate from the Miocene of Pakistan:
838 Description and preliminary analyses. Proc. Natl. Acad. Sci. USA 112, 82-87.

839 Moyà-Solà, S., Köhler, M., 1996. A *Dryopithecus* skeleton and the origin of great-ape
840 locomotion. Nature 379, 156-159.
841 Moyà-Solà, S., Köhler, M., Rook, L., 1999. Evidence of hominid-like precision grip
842 capability in the hand of the Miocene ape *Oreopithecus*. Proc. Natl. Acad. Sci.
843 USA 96, 313-317.
844 Moyà-Solà, S., Köhler, M., Alba, D.M., Casanovas-Vilar, I., Galindo, J., Robles, J.M.,
845 Cabrera, L., Garcés, M., Almécija, S., Beamud, E., 2009. First partial face and
846 upper dentition of the Middle Miocene hominoid *Dryopithecus fontani* from
847 Abocador de Can Mata (Vallès-Penedès Basin, Catalonia, NE Spain): Taxonomic
848 and phylogenetic implications. Am J. Phys. Anthropol. 139, 126-145.
849 Nakano, Y., Ogihara, N., Makishima, H., Shimizu, D., Kagaya, M., Kunimatsu, Y.,
850 Ishida, H., 2004. The locomotor adaptation in the pelvic morphology of
851 *Nacholapithecus*. Anthropol. Sci. 112, 301.
852 Nakatsukasa, M., 2008. Comparative study of Moroto vertebral specimens. J. Hum.
853 Evol. 55, 581-588.
854 Nakatsukasa, M., Kunimatsu, Y., 2009. *Nacholapithecus* and its importance for
855 understanding hominoid evolution. Evol. Anthropol. 18, 103-119.
856 Nakatsukasa, M., Yamanaka, A., Kunimatsu, Y., Shimizu, D., Ishida, H., 1998. A
857 newly discovered *Kenyapithecus* skeleton and its implications for the evolution of
858 positional behavior in Miocene East African hominoids. J. Hum. Evol. 34, 657-
859 664.
860 Nakatsukasa, M., Tsujikawa, H., Shimizu, D., Takano, T., Kunimatsu, Y., Nakano, Y.,
861 Ishida, H., 2003a. Definitive evidence for tail loss in *Nacholapithecus*, an East
862 African Miocene hominoid. J. Hum. Evol. 45, 179-186.

Nakatsukasa, M., Kuminatsu, Y., Nakano, Y., Takano, T., Ishida, H., 2003b. Comparative and functional anatomy of phalanges in *Nacholapithecus kerioi*, a Middle Miocene hominoid from northern Kenya. Primates 44, 371-412.

Nakatsukasa, M., Ward, C.V., Walker, A., Teaford, M.F., Kunimatsu, Y., Ogihara, N., 2004. Tail loss in *Proconsul heseloni*. J. Hum. Evol. 46, 777-784.

Nakatsukasa, M., Kunimatsu, Y., Nakano, Y., Ishida, H., 2007a. Vertebral morphology of *Nacholapithecus kerioi* based on KNM-BG 35250. J. Hum. Evol. 52, 347-369.

Nakatsukasa, M., Kunimatsu, Y., Nakano, Y., Egi, N., Ishida, H., 2007b. Postcranial bones of infant *Nacholapithecus*: Ontogeny and positional behavioral adaptation. Anthropol. Sci. 115, 201-213.

Nakatsukasa, M., Kunimatsu, Y., Shimizu, D., Nakano, Y., Kikuchi, Y., Ishida, H., 2012. Hind limb of the *Nacholapithecus kerioi* holotype and implications for its positional behavior. Anthropol. Sci. 120, 235-250.

Ogihara, N., Almécija, S., Nakatsukasa, M., Nakano, Y., Kikuchi, Y., Kunimatsu, Y., Makishima, H., Shimizu, D., Takano, T., Tsujikawa, H., Kagaya, M., Ishida, H., 2016. Carpal bones of *Nacholapithecus kerioi*, a Middle Miocene Hominoid from Northern Kenya. Am J. Phys. Anthropol. 160, 469-482.

Pickford, M., Ishida, H., Nakaya, Y., Yasui, K., 1987. The Middle Miocene fauna from the Nachola and Aka Aiteputh Formations, Northern Kenya. Afr. Study Monogr. Suppl. Issue 5, 141-154.

Pickford, M., Senut, B., Gommery, D., Treil, J., 2002. Bipedalism in *Orrorin tugenensis* revealed by its femora. Comptes Rendus Palevol. 1, 191-203.

Pilbeam, D.R., Young, D.L., 2001. *Sivapithecus* and hominoid evolution: Some brief comments. In: de Bonis, L., Koufos, G.D., Andrews, P. (Eds.), Hominoid Evolution and Climatic Change in Europe, Vol. 2. Phylogeny of the Neogene

888 Hominoid Primates of Eurasia. Cambridge University Press, Cambridge, pp. 349-
889 364.
890 Pilbeam, D.R., Rose, M.D., Badgley, C., Lipschutz, B., 1980. Miocene hominoids from
891 Pakistan. Postilla 181, 1-94.
892 Pina, M., 2016. Unravelling the positional behaviour of fossil hominoids:
893 Morphofunctional and structural analysis of the primate hindlimb. Ph.D.
894 Dissertation, Universitat Autònoma de Barcelona.
895 Pina, M., Alba, D.M., Almécija, S., Fortuny, J., Moyà-Solà, S., 2012. Paleobiological
896 inferences on the locomotor repertoire of extinct hominoids based on femoral
897 neck cortical thickness: The fossil Great ape *Hispanopithecus laietanus* as a test-
898 case study. Am J. Phys. Anthropol. 149, 142-148.
899 Pina, M., Almécija, S., Alba, D.M., O'Neill, M.C., Moyà-Solà S., 2014. The Middle
900 Miocene ape *Pierolapithecus catalaunicus* exhibits extant great ape-like
901 morphometric affinities on its patella: Inferences on knee function and evolution.
902 PLoS One 9, e91944.
903 Pina, M., Kikuchi, Y., Nakatsukasa, M., Nakano, Y., Kunimatsu, Y., Ogihara, N.,
904 Shimizu, D., Takano, T., Tsujikawa, H., Ishida, H., 2018. Revisiting the femoral
905 morphology of *Nacholapithecus kerioi*. Anthropol. Sci. 126 (3): 188.
906 Pina, M., Alba, D.M., Moyà-Solà, S., Almécija, S., 2019. Femoral neck cortical bone
907 distribution of dryopithecin apes and the evolution of hominid locomotion. J.
908 Hum. Evol. 136, 102651.
909 Pina, M., DeMiguel, D., Puigvert, F., Marcé-Nogué, J., Moyà-Solà S., 2020. Knee
910 function through finite element analysis and the role of Miocene hominoids to
911 understand the origin of antipronograde behaviours: The *Pierolapithecus*
912 *catalaunicus* patella as a test-case study. Palaeontology 63, 459-475.

913 R Core Team, 2017. R: A language and environment for statistical computing. R
914 Foundation for Statistical Computing, Vienna.
915 Raza, S.M., Barry, J.C., Pilbeam, D., Rose, M.D., Shah, S.M.I., Ward, S., 1983. New
916 hominoid primates from the middle Miocene Chinji Formation, Potwar Plateau,
917 Pakistan. Nature 306, 52-54.
918 Richmond, B.G., Whalen, M., 2001. Forelimb function, bone curvature and phylogeny
919 of *Sivapithecus*. In: de Bonis, L., Koufos, G.D., Andrews, P. (Eds.), Hominoid
920 Evolution and Climatic Change in Europe, Vol. 2. Phylogeny of the Neogene
921 Hominoid Primates of Eurasia. Cambridge University Press, Cambridge, pp. 326-
922 348.
923 Richmond, B.G., Jungers, W.L., 2008. *Orrorin tugenensis* femoral morphology and the
924 evolution of hominin bipedalism. Science 319, 1662-1665.
925 Rook, L., Renne, P., Benvenuti, M., Papini, M., 2000. Geochronology of *Oreopithecus*-
926 bearing succession at Baccinello (Italy) and the extinction pattern of European
927 Miocene hominoids. J. Hum. Evol. 39, 577-582.
928 Rose, M.D., 1983. Miocene hominoid postcranial morphology. Monkey-like, ape-like,
929 neither, or both?. In: Ciochon, R.L., Corruccini, R.S. (Eds.), New Interpretations
930 of Ape and Human Ancestry. Plenum Press, New York, pp. 503-516.
931 Rose, M.D., 1986. Further hominoid postcranial specimens from late Miocene Nagri
932 Formation of Pakistan. J. Hum. Evol. 15, 333-367.
933 Rose, M.D., 1993. Locomotor anatomy of Miocene hominoids. In: Gebo, D.L. (Ed.),
934 Postcranial Adaptation in Nonhuman Primates. Northern Illinois University Press,
935 Dekalb, pp. 252-272.
936 Rose, M.D., Nakano, Y., Ishida, H., 1996. *Kenyapithecus* postcranial specimens from
937 Nachola, Kenya. Afr. Study Monogr. Suppl. 24, 3-56.

938 Ruff, C., 1988. Hindlimb articular surface allometry in hominoidea and *Macaca*, with
939 comparisons to diaphyseal scaling. J. Hum. Evol. 17, 687-714.
940 Sawada, Y., Pickford, M., Itaya, T., Makinouchi, T., Tateishi, M., Kabeto, K., Ishida,
941 S., Ishida, H., 1998. K-Ar ages of miocene hominoidea (*Kenyapithecus* and
942 *Samburupithecus*) from Samburu Hills, Northern Kenya. C. R. Acad. Sci. IIA
943 Earth Planet. Sci. 326, 445-451.
944 Schindelin, J., Arganda-Carreras, I., Frise, E., Kaynig, V., Longair, M., Pietzsch, T.,
945 Preibisch, S., Rueden, C., Saafeld, S., Schmid, B., Tinevez, J.-Y., White, D. J.,
946 Hartenstein, V., Eliceiri, K., Tomancak, P., Cardona, A., 2012. Fiji: An open-
947 source platform for biological-image analysis. Nat. Methods 9, 676-682.
948 Senut, B., 2016. Morphology and environment in some fossil hominoids and pedetids
949 (Mammalia). J. Anat. 228, 700-715.
950 Senut, B., Pickford, M., Gommery, D., Kunimatsu, Y., 2000. A new genus of Early
951 Miocene hominoid from East Africa: *Ugandapithecus major* (Le Gros Clark &
952 Leakey, 1950). C. R. Acad. Sci. IIA Earth Planet. Sci. 331, 227-233.
953 Senut, B., Pickford, M., Gommery, D., Mein, P., Cheboi, K., Coppens, Y., 2001. First
954 hominid from the Miocene (Lukeino Formation, Kenya). C. R. Acad. Sci. IIA
955 Earth Planet. Sci. 332, 137-144.
956 Senut, B., Nakatsukasa, M., Kunimatsu, Y., Nakano, Y., Takano, T., Tsujikawa, H.,
957 Shimizu, D., Kagaya, M., Ishida, H., 2004. Preliminary analysis of
958 *Nacholapithecus* scapula and clavicle from Nachola, Kenya. Primates 45, 97-104.
959 Stern, Jr., J.T., 1972. Anatomical and functional specializations of the human gluteus
960 maximus. Am J. Phys. Anthropol. 36, 315-339.

961 Stern, Jr., J.T., Susman, R.L., 1981. Electromyography of the gluteal muscles in
962 *Hylobates*, *Pongo*, and *Pan*: Implications for the evolution of hominid bipedality,
963 Am J. Phys. Anthropol. 55, 153-66.
964 Straus, W.L., Jr., 1963. The classification of *Oreopithecus*. In: Washburn, S.L. (Ed.),
965 Classification and Human Evolution. Aldine, Chicago, pp. 146-177.
966 Sukhdeo, S., Parsons, J., Niu, X.M., Ryan, T.M., 2019. Trabecular bone structure in the
967 distal femur of humans, apes, and baboons. Anat. Rec. doi:10.1002/ar.24050.
968 Susman, R.L., 2004. *Oreopithecus bambolii*: An unlikely case of hominidlike grip
969 capability in a Miocene ape. J. Hum. Evol. 46, 105-117.
970 Takano, T., Nakatsukasa, M., Kunimatsu, Y., Nakano, Y., Ishida, H., 2003. Functional
971 morphology of the *Nacholapithecus* forelimb long bones. Am J. Phys. Anthropol.
972 120, 205-206.
973 Takano, T., Nakatsukasa, M., Kunimatsu, Y., Nakano, Y., Ogihara, N., Ishida, H., 2018.
974 Forelimb long bones of *Nacholapithecus* (KNM-BG 35250) from the middle
975 Miocene in Nachola, northern Kenya. Anthropol. Sci. 126, 135-149.
976 Takano, T., Nakatsukasa, M., Pina, M., Kunimatsu, Y., Nakano, Y., Morimoto,
977 N., Ogihara, N., Ishida, H., In press. New forelimb long bone specimens
978 of *Nacholapithecus kerioi* from the Middle Miocene of northern
979 Kenya. Anthropol. Sci. 128.
980 Ward, C.V., 2015. Postcranial and locomotor adaptations of hominoids. In: Henke, W.,
981 Tattersall, I. (Eds.), Handbook of Paleoanthropology. Springer, Berlin Heidelberg,
982 pp. 1363-1386.
983 Ward, C.V., Walker, A., Teaford, M.F., Odhiambo, I., 1993. Partial skeleton of
984 *Proconsul nyanzae* from Mfangano Island, Kenya. Am J. Phys. Anthropol. 90, 77-
985 111.

Ward, C.V., Ruff, C.B., Walker, A., Teaford, F., Rose, M.D., Nengo, I.O., 1995. Functional morphology of *Proconsul* patellas from Rusinga Island, Kenya, with implications for other Miocene-Pliocene catarrhines. J. Hum. Evol. 29, 1-19.

Ward, C.V., Hammond, A.S., Plavcan, J.M., Begun, D.R., 2019. A late Miocene hominid partial pelvis from Hungary. J. Hum. Evol., 102645.

Figure captions

Figure 1. Map of the fossil locality of Nachola in Kenya.

Figure 2. Linear measurements taken of the proximal femora for quantitative analyses. A) proximal view; B) posterior view; and C) anterior view. Abbreviations: APN = anteroposterior depth of the femoral neck; SIH = maximum superoinferior height of the femoral head; SIN = minimum superoinferior height of the femoral neck; NL = femoral neck length (between the most lateral edge of the femoral head to the medialmost limit of the trochanteric crest); NSangle = femoral neck-shaft angle; TotW = total mediolateral width of the proximal femur from the medialmost point of the femoral head to the lateralmost point of the greater trochanter. Modified from Pina, 2016.

Figure 3. Proximal fossil femoral fragments used for comparisons with *Nacholapithecus kerioi* (anterior view). When available, the distal portion is also displayed (anterior view above, posterior view below). A) *Morotopithecus bishopi* (UMP MORII 94’80); B) *Proconsul major* (combination of NAP IX 46’99, NAP IX B 64, NAP IX 65 P. 67 fragments; reversed); C) *Turkanapithecus kalakolensis* (KNM-WK 16950I); D) *Ekembo nyanzae* (KNM-MW 13142A); E) *Ekembo nyanzae* (KNM-RU 5527; reversed); F) *Equatorius africanus* (BMNH M.16331; reversed; pictures from

cast); G) *Dryopithecus fontani* (IPS 41724); and H) *Hispanopithecus laietanus* (IPS 18800.29). Femora are displayed with the same maximum superoinferior height of the femoral head (SIH) to facilitate morphological comparisons. Dashed lines at the right bottom of A, C, and E represent the outline of the patellar groove. Scale bars = 20 mm.

Figure 4. Fossil femoral fragments belonging to *Nacholapithecus kerioi* described in this work (A–P). KNM-BG 17778 (A, anterior view; B, posterior view); KNM-BG 40844 (C, anterior view; D, posterior view); KNM-BG 40964 (E, anterior view; F, posterior view); KNM-BG 42757 (G, proximal; H, anterior; I, medial; and J, posterior views); KNM-BG 44953B (K, anterior; L, medial; and M, posterior views); and KNM-BG; 42779 (N, anterior; O, side; and P, posterior views). Scale bar = 20 mm.

Figure 5. Fossil femoral fragments belonging to *Nacholapithecus kerioi* described in this study. These remains are associated with the same individual (probably an immature). A–C) KNM-BG 42738/42756C (proximal fragment); D–E) KNM-BG 42722 (shaft fragment); F–I) KNM-BG 42732 (distal fragment). A, I) proximal views; B, D, F) anterior views; C, E, G) posterior views; H) distal view. Black arrows denote (A) the absence of anteversion of the head, (C) the intertrochanteric line, and (F) the most proximal point of the lateral and medial rims of the patellar groove. Dashed white lines denote the supracondylar ridges (E). Dashed black line represents the square-shaped outline of the patellar groove (F). Scale bar = 20 mm.

Figure 6. Boxplots showing (A) the relative size of the head index: SIH/(ÖSIN*APN) (SIH = superoinferior height of the femoral head; SIN = superoinferior height of the femoral neck; APN = anteroposterior depth); (B) the relative neck length (RelativeNL);

and (C) neck-shaft angle (NSangle). Vertical lines represent the median, boxes the interquartile range, IQR (between the 25th and the 75th percentiles), whiskers the 1.5*IQR, and circles the outliers. Colors represent major taxonomic groups: dark green, African apes; light green, Asian apes; yellow, cercopithecines; orange, colobines; dark blue, atelids; light blue, cebines (for colors see online version).

Figure 7. *Nacholapithecus kerioi* femoral fragments showing some of the anatomical features discussed in the text. A) KNM-BG 38391A (anterior view); B) KNM-BG 44953A (anterior view); C) KNM-BG 48093 (anterior view); D–E) KNM-BG 17816 (D, anterior view; E, posterior view); F–G) KNM-BG 44954A (F, posterior view; G, lateral view); H) KNM-BG 35250A (holotype; anterior view); I) KNM-BG 35250J (holotype; anterior view); J) AMNH 103659, *Macaca fascicularis* (anterior view) ; K) AMNH 103344, *Hylobates klossi* (anterior view); L) AMNH 86857, *Pan paniscus* (anterior view). J–L are depicted at the same femoral length (from the head to the distal end). A–B) differences in greater trochanter lateral flare (fragments scaled to the same superoinferior height of the femoral head). A, C) sexual dimorphism: C, smallest femur belonging to a female (Kikuchi et al., 2018); its small size can be compared with A, the largest male femur (except for H; Kikuchi et al., 2018). A and C femoral fragments are depicted to the same scale. D–E) lesser trochanter close to the femoral neck; F–G) marked gluteal tuberosity close to the greater trochanter. I) square-shaped patellar groove. Black arrows highlight the referenced anatomical traits. Scale bar = 20 mm.


SOUTH SUDAN
ETHIOPIA
Lake Turkana
UGANDA
Nachola
SOMALIA
Maralal
KENYA
Nakuru
Lake Victoria
Nairobi
TANZANIA
INDIAN OCEAN
N
0
200 km

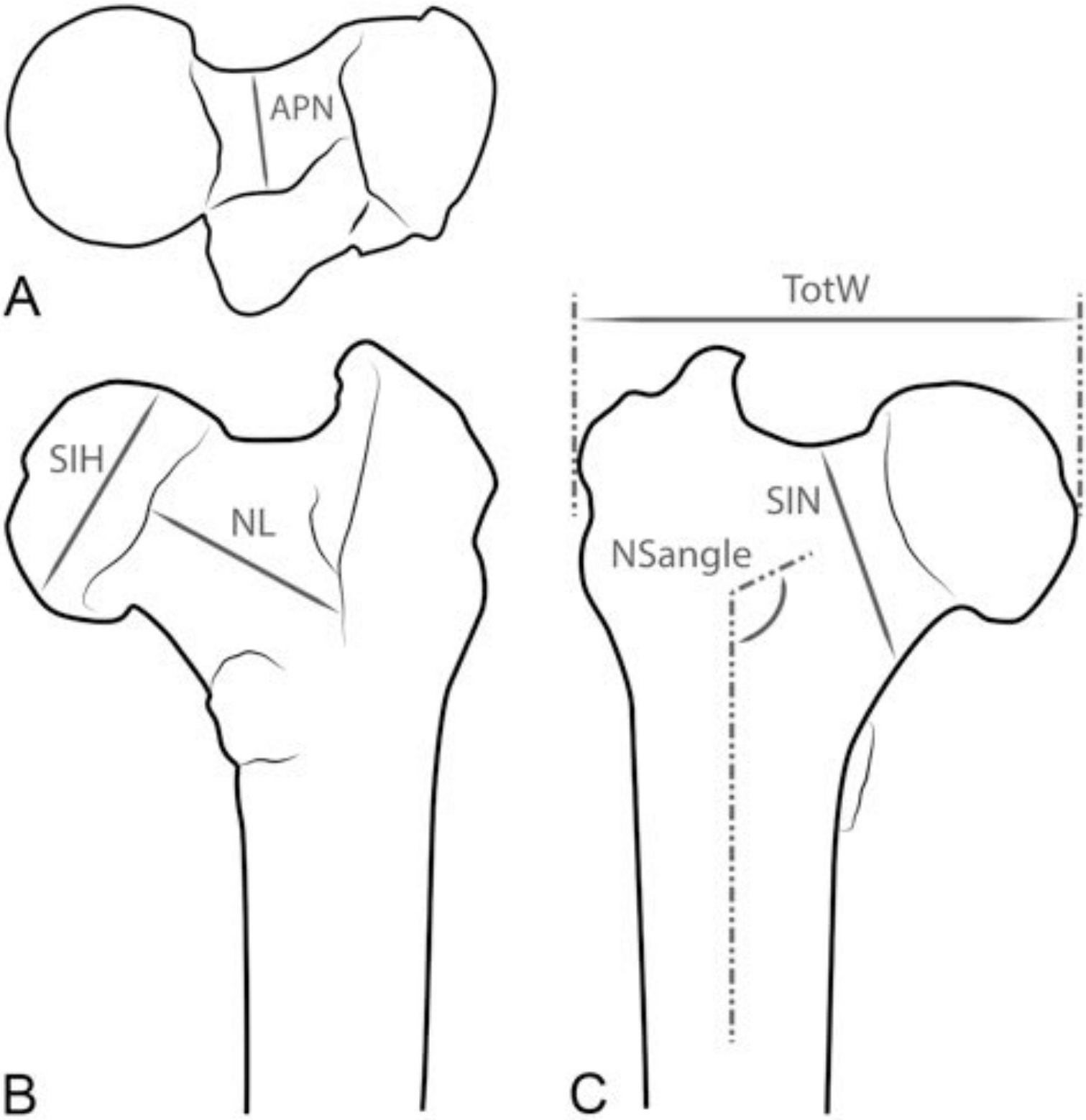
APN
A
SIH
NL
B
TotW
SIN
NSangle
C


A
M. bishopi
B
P. major
C
T. kalakolensis
D
Ek. nyanzae
E
Ek. nyanzae
F
Eq. africanus
G
D. fontani
H
H. laietanus


KNM-BG 17778
A
B
KNM-BG 40844
C
D
KNM-BG 40964
E
F
KNM-BG 42757
G
H
I
J
KNM-BG 44953B
K
L
M
KNM-BG 42779
N
O
P

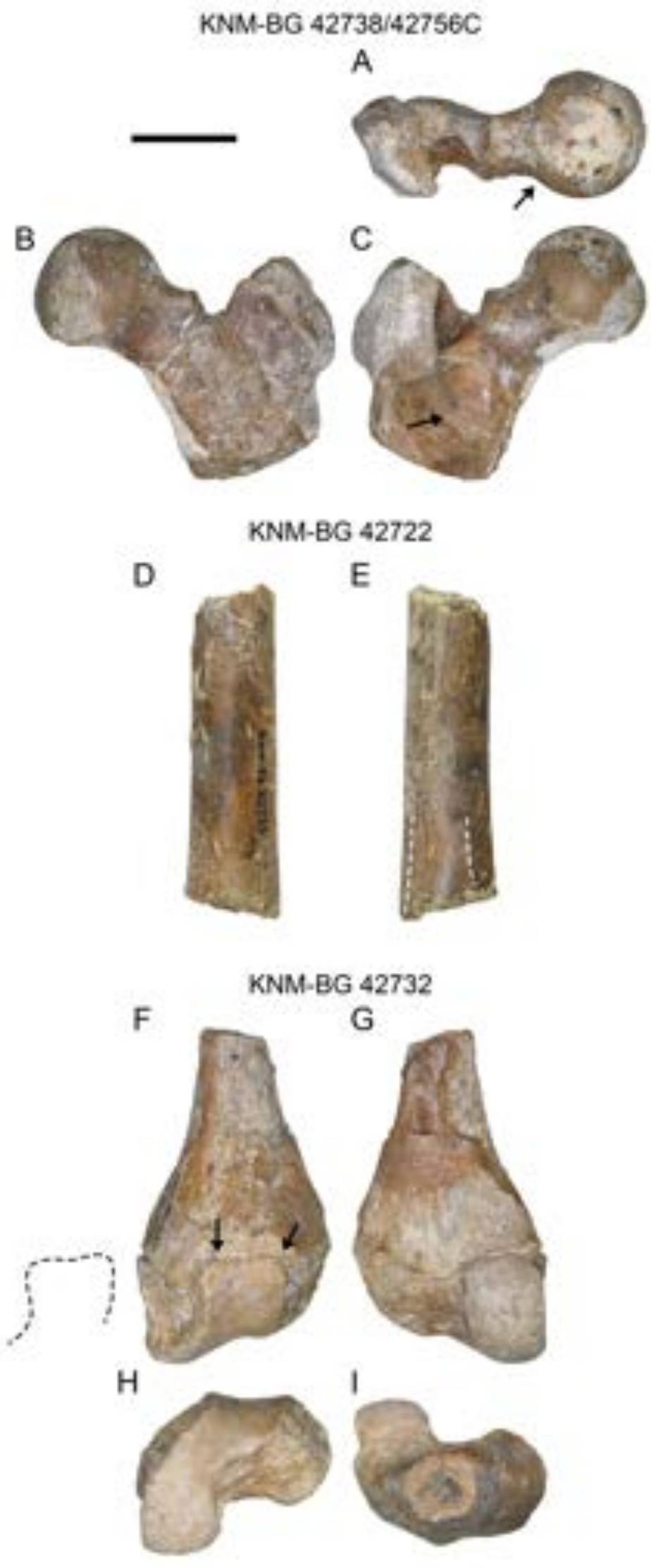
KNM-BG 42738/42756C
A
B
C
KNM-BG 42722
D
E
KNM-BG 42732
F
G
H
I

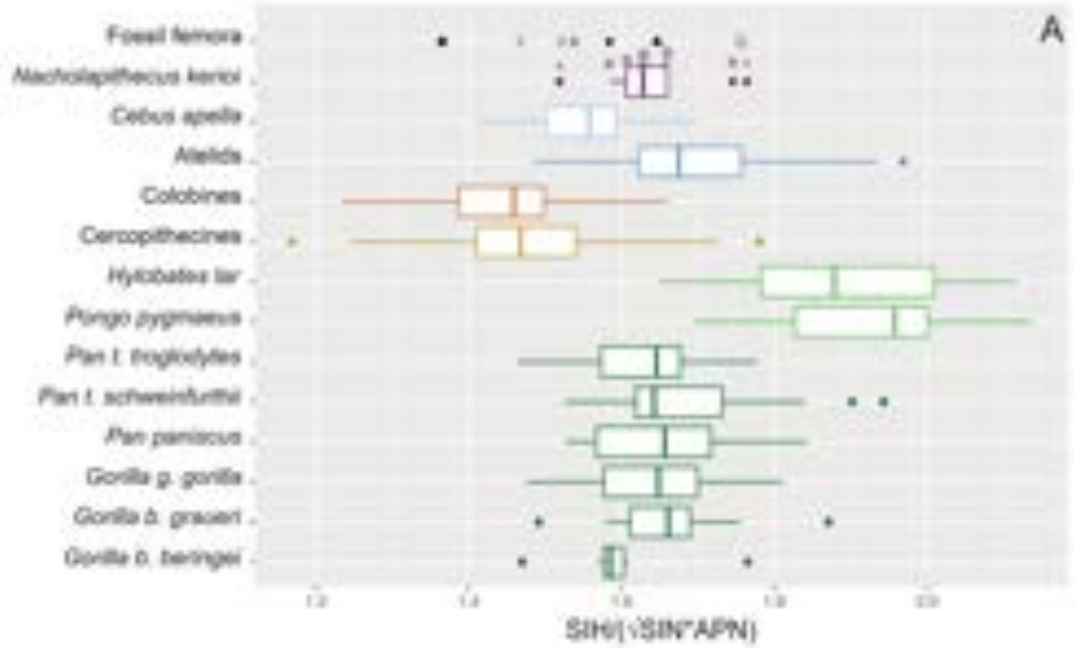
A
Fossil femora
Nacholapithecus kerioi
Cebus apella
Atelids
Colobines
Cercopithecines
Hylobates lar
Pongo pygmaeus
Pan t. troglodytes
Pan t. schweinfurthii
Pan paniscus
Gorilla g. gorilla
Gorilla b. graueri
Gorilla b. beringei
SIH/(√SIN*APN)

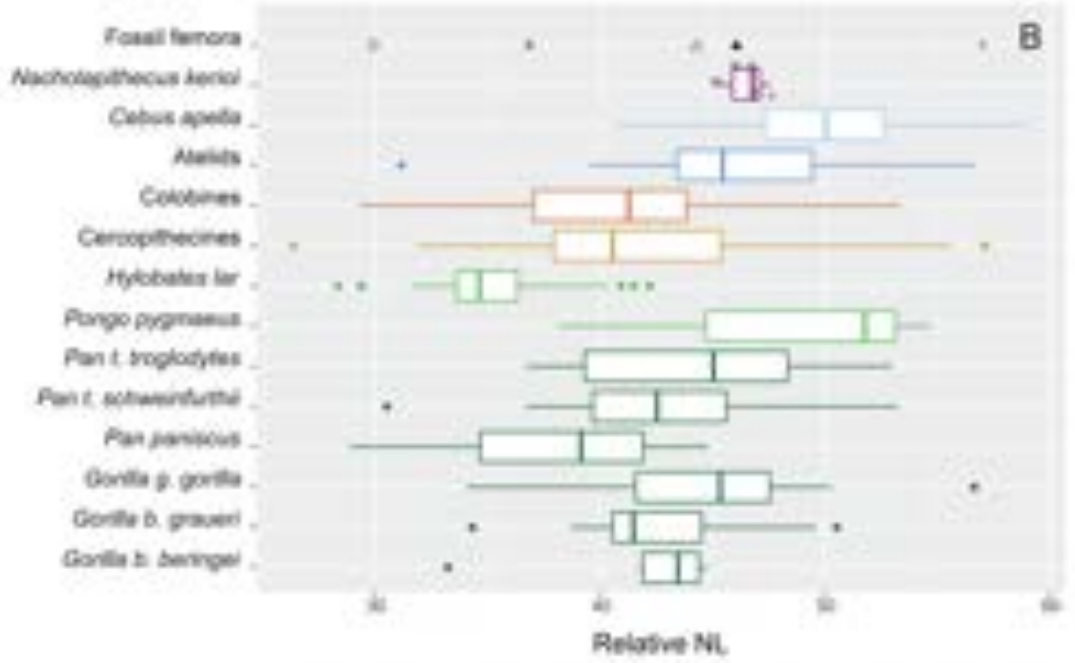
B
Fossil femora
Nacholapithecus kerioi
Cebus apella
Atelids
Colobines
Cercopithecines
Hylobates lar
Pongo pygmaeus
Pan t. troglodytes
Pan t. schweinfurthii
Pan paniscus
Gorilla g. gorilla
Gorilla b. graueri
Gorilla b. beringei
Relative NL

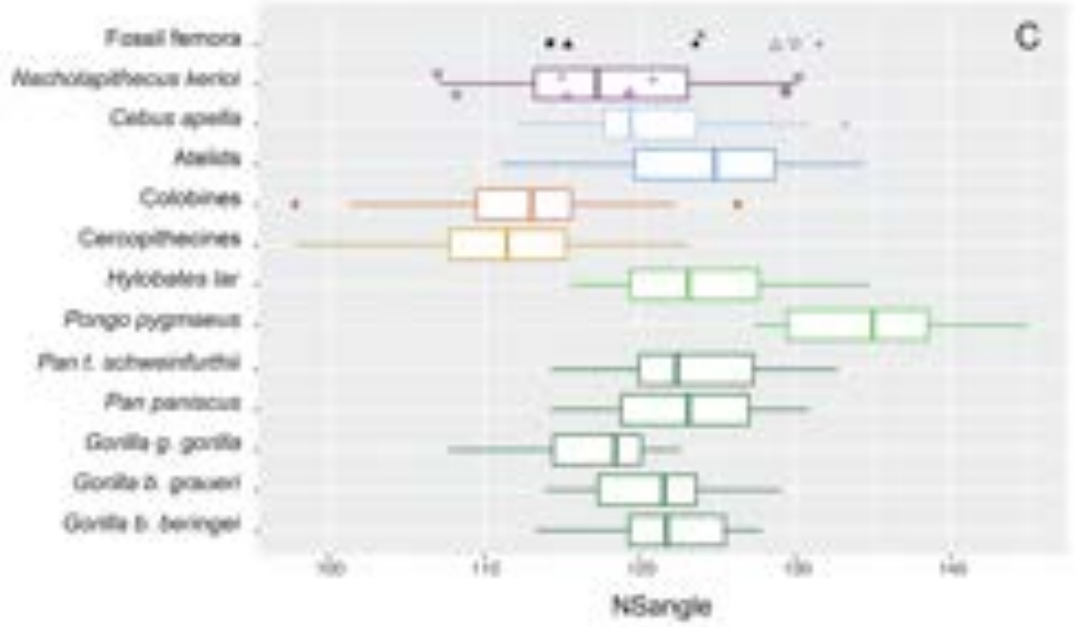
C
Fossil femora
Nacholapithecus kerioi
Cebus apella
Atelids
Colobines
Cercopithecines
Hylobates lar
Pongo pygmaeus
Pan t. schweinfurthii
Pan paniscus
Gorilla g. gorilla
Gorilla b. graueri
Gorilla b. beringei
NSangle


N. kerioi (KNM-BG 35250A)
N. kerioi females
N. kerioi males
Eg. africanus (BMNH M16331)
Ek. nyanzae (KNM-BG 13142A)
Ek. nyanzae (KNM-RU 5527)
T. kalakolensis (KNM-WK 16950)
P. major (NAP IX 46'99)
M. bishopi (UMP MORB 94'80)
D. fontani (IPS 41724)
H. laetanus (IPS 18800.29)

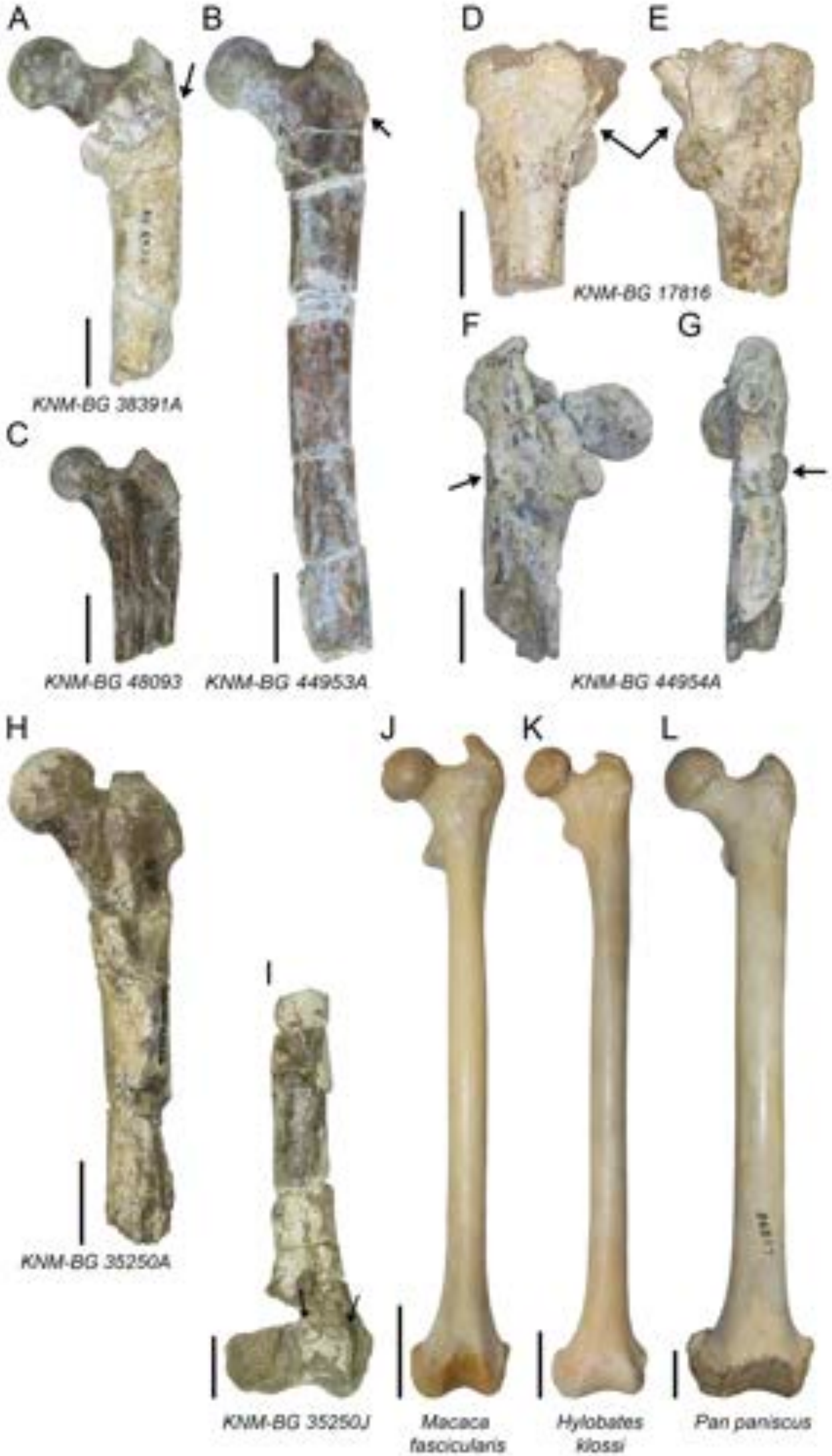
A
B
D
E
KNM-BG 38391A
KNM-BG 17816
C
F
G
KNM-BG 48093
KNM-BG 44953A
KNM-BG 44954A
H
I
J
K
L
KNM-BG 35250A
KNM-BG 35250J
Macaca fascicularis
Hylobates klossi
Pan paniscus

Table 1

Femoral remains attributed to *Nacholapithecus kerioi*. Sex is provided for those specimens included in the sexual dimorphism analysis in Kikuchi et al. (2018).[a]

Accession number	Description	Side	Sex	Locality	First reference	APN	SIH	SIN	NL	TotW	NSangle
KNM-BG 17775	Head with neck	?		BG-X	Rose et al. (1996)						
KNM-BG 17778	Head	?L		BG-X	This study[b]						
KNM-BG 17816	Proximal shaft, including LT	R		BG-I	Rose et al. (1996)						
KNM-BG 17819	Head with neck	R		BG-I	Rose et al. (1996)						
KNM-BG 17820	Proximal fragment	L		BG-I	Rose et al. (1996)						
KNM-BG 17821	Head with neck	?		BG-I	Rose et al. (1996)						
KNM-BG 35250A	Proximal half	R	M	BG-K	Nakatsukasa et al. (1998)[c]	12.1	22.3	15.5			129.4
KNM-BG 35250B	Distal fragment	R		BG-K	Nakatsukasa et al. (1998)						
KNM-BG 35250D	Proximal fragment	L		BG-K	Nakatsukasa et al. (1998)						
KNM-BG 35250J	Shaft and distal end	L		BG-K	Nakatsukasa et al. (1998)						
KNM-BG 35250U	Proximal fragment	L		BG-K	Nakatsukasa et al. (1998)						
KNM-BG 38391A	Proximal fragment	L	M	BG-K	Kikuchi et al. (2018)[c]	9.6	22.0	16.2	23.4	49.7	115.3
KNM-BG 40794A	Head with neck	R	F	BG-K	Kikuchi et al. (2018)[c]	7.8	18.5	14.5			

KNM-BG 40826	Proximal fragment	R	F	BG-K	Kikuchi et al. (2018)[c]	8.9	17.3	13.4			130.1
KNM-BG 40844	Head	?R		BG-K	This study						
KNM-BG 40933	Head with neck	L	M	BG-K	Kikuchi et al. (2018)[c]	12.3	21.9	16.9			
KNM-BG 40964	Proximal fragment without head and neck	R		BG-K	This study						
KNM-BG 42713A	Proximal half	L	F	BG-K	Kikuchi et al. (2018)[c]						
KNM-BG 42722	Shaft fragment	R		BG-I	This study						
KNM-BG 42732	Distal fragment	L		BG-I	This study						
KNM-BG 42738/42756C	Proximal fragment	L	M	BG-I West	Kikuchi et al. (2018)[c]	12.9	24.2	16.5	25.8	54.2	121.0
KNM-BG 42757	Proximal fragment	L		BG-K	This study[b]						114.9
KNM-BG 42779	Shaft fragment (distal)	L		BG-K	This study						
KNM-BG 44953A	Proximal fragment	R	F	BG-K	Kikuchi et al. (2018)[c]	8.1	17.1	13.1	17.3	37.7	108.3
KNM-BG 44953B	Proximal fragment without head and neck	L		BG-K	This study						
KNM-BG 44954A	Proximal fragment	L	M	BG-K	Kikuchi et al. (2018)[c]						
KNM-BG 48092A	Proximal fragment	R	F	BG-K	Kikuchi et al. (2018)[c]	9.1	18.0	13.8	18.0	38.5	119.2
KNM-BG 48093	Proximal fragment	L	F	BG-K	Kikuchi et al. (2018)[c]	8.2	17.0	13.3	17.3	38.3	107.1

Abbreviations: APN = anteroposterior depth of the femoral neck (mm); BG = Baragoi; F = female; L = left; LT = lesser trochanter; M = male; NL = neck length (mm); NSangle = neck-shaft angle (degrees); R = right; SIH = superoinferior height of the femoral head (mm); SIN = superoinferior height of the femoral neck (mm); TotW = total mediolateral width of the proximal femur from the medialmost point of the femoral head to the lateral-most point of the greater trochanter (mm); ? = uncertain.

[a] These femoral fragments are fully open access for further analytical studies.

[b] Used for comparative purposes (Ishida et al., 2004; Nakatsukasa et al., 2012), but never formally described.

[c] Fragment included in the quantitative analyses.

Table 2

Extant anthropoid taxa included in the analyses. Number of females/males/unknown sex in parentheses.[a]

	n		
Species	SIH/(ÖSIN*APN)	Relative NL	NSangle
Cebus apella	33 (13/20/-)	27 (12/15/-)	27 (12/15/-)
Ateles sp.	8 (5/2/1)	8 (2/2/4)	8 (2/2/4)
Alouatta sp.	45 (22/19/4)	28 (15/8/5)	30 (14/10/6)
Presbytis sp.	34 (20/14/-)	25 (14/11/-)	33 (16/17-/)
Colobus sp.	28 (13/15/-)	32 (12/18/2)	27 (12/14/1)
Nasalis larvatus	25 (12/13/-)	25 (12/13/-)	25 (12/13/-)
Chlorocebus sp.	16 (6/8/2)	10 (4/5/1)	—
Cercopithecus sp.	49 (19/30/-)	37 (11/20/6)	14 (5/8/1)
Macaca sp.	30 (15/15/-)	27 (13/14/-)	26 (13/13/-)
Lophocebus sp.	15 (2/12/1)	7 (1/5/1)	—
Mandrillus sp.	13 (4/8/1)	10 (3/6/1)	10 (3/6/1)
Papio sp.	25 (5/11/9)	18 (2/8/8)	20 (4/9/7)
Hylobates lar	26 (13/13/-)	25 (12/13/-)	26 (13/13/-)
Pongo pygmaeus	12 (4/5/3)	11 (5/4/2)	12 (4/5/3)
Pan t. troglodytes	29 (14/15/-)	17 (4/9/4)	—
Pan t. schweinfurthii	25 (8/17/-)	21 (7/10/4)	26 (8/16/2)
Pan paniscus	20 (11/9/-)	20 (11/9/-)	20 (11/9/-)
Gorilla g. gorilla	31 (13/18/-)	20 (10/10/-)	26 (13/13/-)
Gorilla b. graueri	21 (8/13/-)	22 (8/14/-)	21 (8/13/-)
Gorilla b. beringei	10 (5/5/-)	7 (4/3/-)	8 (4/4/-)

Abbreviations: APN = anteroposterior depth of the femoral neck; *n* = sample size; NL = neck length; NSangle = neck-shaft angle; SIH = superoinferior height of the femoral head; SIN = superoinferior height of the femoral neck.

[a] Data for these femora were collected at the American Museum of Natural History, New York (AMNH, USA), the Museum of Comparative Zoology, Harvard University (MCZ, USA), Peabody Museum of Archaeology and Ethnology, Harvard University (PBMA, USA), and the Royal Museum of Central Africa (RMCA, Belgium).

Table 3

Descriptive statistics for the SIH/(ÖSIN*APN) index, relative NL, and NSangle variables in the *Nacholapithecus kerioi* sample.

	n	Mean	SD	Min	Max
SIH/(ÖSIN*APN)	9	1.644	0.076	1.519	1.764
Relative NL	5	46.50	0.969	45.17	47.60
NSangle	8	118.2	8.587	107.1	130.1

Abbreviations: APN = anteroposterior neck depth; *n* = sample size; Max = maximum value; Min = minimum value; NL = neck length; NSangle = neck-shaft angle; SIH = superoinferior height of the femoral head; SIN = superoinferior height of the femoral neck; SD = standard deviation.

Table 4

Post-hoc pairwise comparisons between *Nacholapithecus kerioi* and extant anthropoids for the SIH/(ÖSIN*APN) index, relative NL, and NSangle.[a]

	Nacholapithecus kerioi		
	SIH/(ÖSIN*APN)	Relative NL	NSangle
Cebus apella	NS	NS	NS
Atelids	NS	NS	**
Colobines	***	*	*
Cercopithecines	**	*	**
Hylobates lar	***	***	*
Pongo pygmaeus	*	NS	***
Pan troglodytes troglodytes	NS	NS	—
Pan troglodytes schweinfurthii	NS	NS	*
Pan paniscus	NS	**	NS
Gorilla gorilla gorilla	NS	NS	NS
Gorilla beringei graueri	NS	NS	NS
Gorilla beringei beringei	NS	NS	NS

Abbreviations: SIH/(ÖSIN*APN) = relative size of the femoral head (APN = anteroposterior neck depth; SIH = superoinferior height of the femoral head; SIN = superoinferior height of the femoral neck); Relative NL = neck length divided by total mediolateral width of the proximal femur multiplied by 100; NSangle = neck-shaft angle of the femur.

[a] NS, no significant differences; *, $p < 0.05$; **, $p < 0.005$; ***, $p < 0.001$.

Supplementary Online Material (SOM):

New femoral remains of *Nacholapithecus kerioi*: Implications for intraspecific variation and Miocene hominoid evolution

Marta Pina[a,b*1], Yasuhiro Kikuchi[c], Masato Nakatsukasa[a], Yoshihiko Nakano[d], Yutaka Kunimatsu[e], Naomichi Ogihara[f], Daisuke Shimizu[g], Tomo Takano[h], Hiroshi Tsujikawa[i], Hidemi Ishida[j]

[a] *Laboratory of Physical Anthropology, Graduate School of Science, Kyoto University, Kyoto 606-8502, Japan*

[b] *Institut Català de Paleontologia Miquel Crusafont, Universitat Autònoma de Barcelona, c/ Columnes s/n, Campus de la UAB, 08193 Cerdanyola del Vallès, Barcelona, Spain*

[c] *Division of Human Anatomy and Biological Anthropology, Department of Anatomy and Physiology, Faculty of Medicine, Saga University, Saga 849-8501, Japan*

[d] *Department of Biological Anthropology, Osaka University, Suita, Osaka 565-8502, Japan*

[e] *Department of Business Administration, Faculty of Business Administration, Ryukoku University, Kyoto, 612-8577, Japan*

[f] *Department of Biological Sciences, Graduate School of Science, The University of Tokyo, Tokyo 113-0033, Japan*

[g] *Faculty of Nursing and Rehabilitation, Chubu Gakuin University, Seki, Gifu, 504-0837, Japan*

[h] *Japan Monkey Centre, Aichi 484-0081, Japan*

[i] *Department of Rehabilitation, Faculty of Medical Science and Welfare, Tohoku Bunka Gakuen University, Sendai 981-8551, Japan*

[1] Present address: *School of Earth and Environmental Sciences, Faculty of Science and Engineering, University of Manchester, Manchester M13 9PL, United Kingdom*

[j] *Professor Emeritus. Kyoto University, Kyoto 606-8502, Japan*

***Corresponding author.**

E-mail address: marta.pinamiguel@manchester.ac.uk (M. Pina)

SOM Figure S1. Comparison of the femoral distal diaphysis fragment (posterior views) of *Nacholapithecus kerioi* (KNM-BG 42722; left) with *Equatorius africanus* (cast BNMH M 16332-3; right). KNM-BG 42722 is placed at the shaft location that might correspond with that of BNMH M 16332-3. Scale bar = 20 mm.

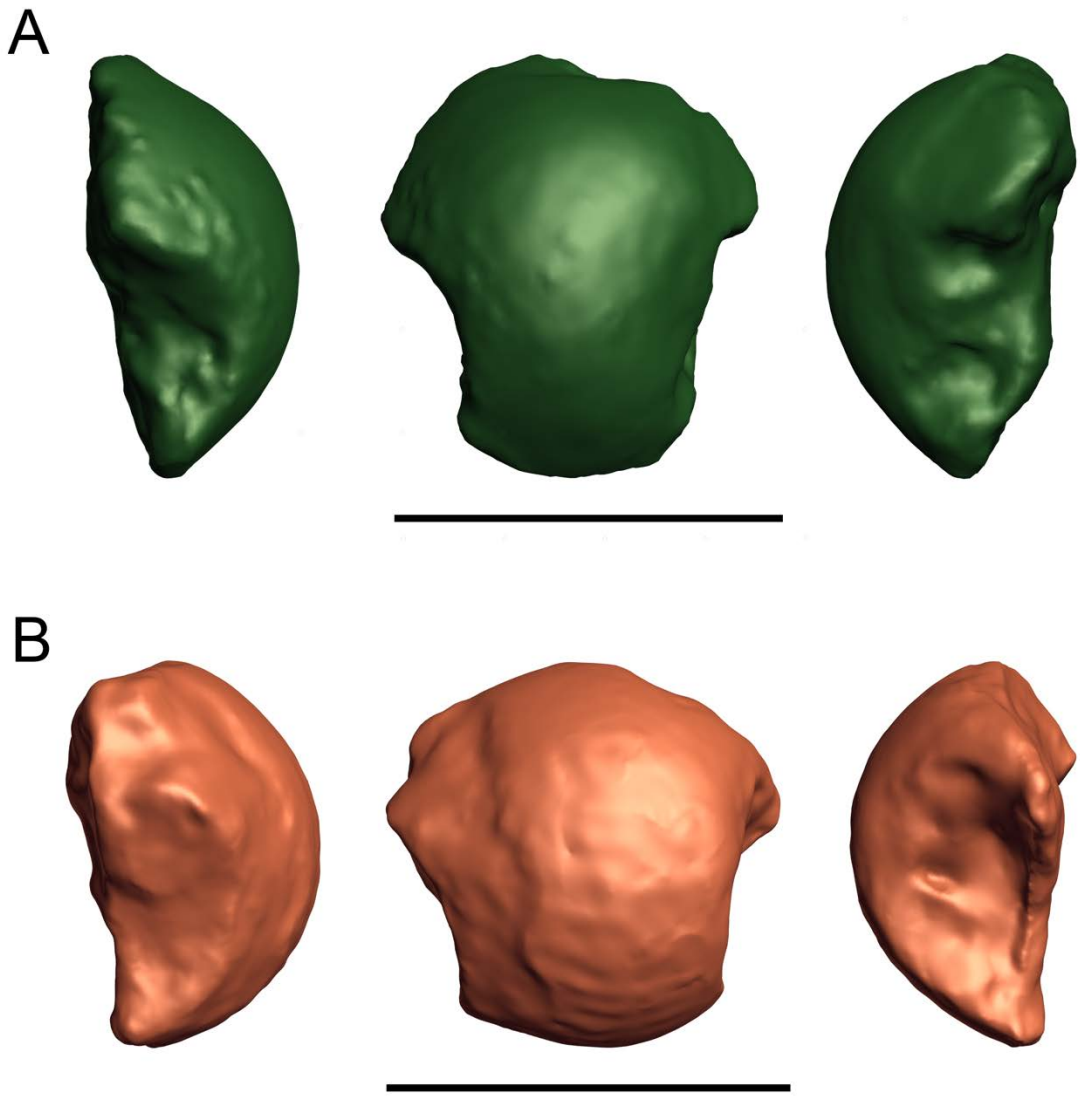

SOM Figure S2. Screenshots from 3D models of A) KNM-BG 15333, and B) KNM-BG 13336. Left and right, side views; center, medial view. These two fragments were described by previous authors (Rose et al., 1996), who suggested that both fragments would be femoral heads of the species *Nacholapithecus kerioi*. We amended these attributions in this work, suggesting that (A) is a humeral head of *N. kerioi;* whereas (B) would be a femoral fragment that belongs to a nonprimate mammal (see text for further explanation). Scale bar = 20 mm.

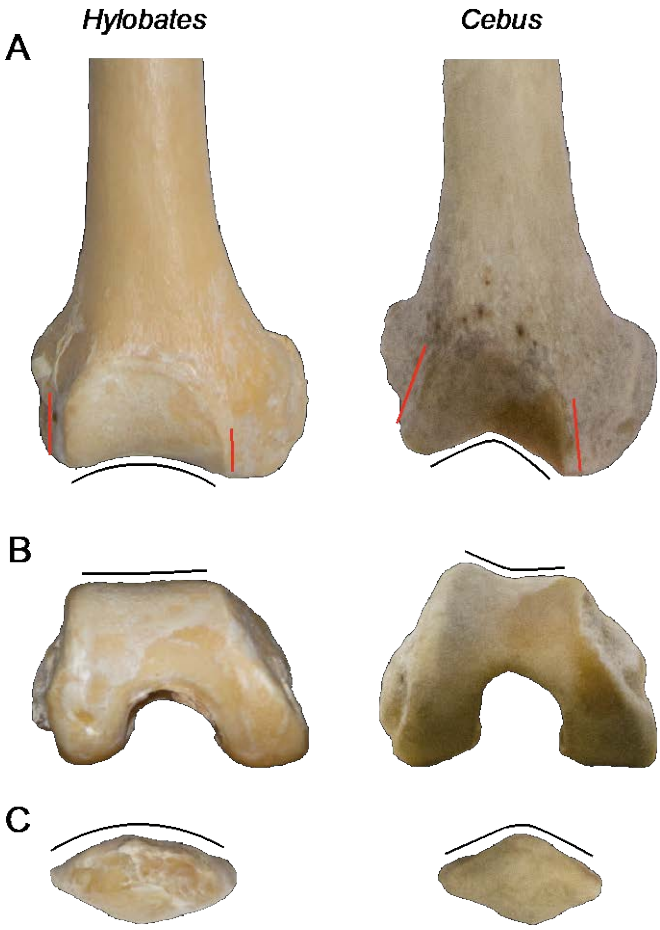

SOM Figure S3. Distal femoral end and patellae of *Hylobates* and *Cebus* in A) anterior, B) distal, and C) proximal views, respectively. Femora are displayed at the same mediolateral width, and patella at the same anteroposterior thickness to facilitate morphological comparisons. Black continuous lines denote the depth of the patellar groove in the femur and its respective morphology at the articular surface of the patella. As shown in the figure, anthropoid monkeys display a deeper patellar groove while it is shallow in apes. Red continuous lines represent the lateral and medial rims of the patellar groove in the femur, highlighting that the rims are parallel in apes and tend to converge in anthropoid monkeys. See also 3D models of femora belonging to *N. kerioi* (KNM-BG 42732), *Hylobates lar*, and *Cebus apella* (SOM 3D Models S1, S2, and S3).

SOM Table S1

Descriptive statistics for APN, SIH, SIN, NL, and TotW in the *Nacholapithecus kerioi* sample. All measurements are taken in mm.

	n	Mean	SD	Min	Max
APN	9	9.89	2.00	7.76	12.90
SIH	9	20.05	3.01	17.00	24.80
SIN	9	14.99	1.76	13.10	18.20
NL	5	20.36	3.97	17.30	25.80
TotW	5	43.68	7.72	37.70	54.20

Abbreviations: APN = anteroposterior neck depth; *n* = sample size; Max = maximum value; Min = minimum value; NL = neck length; SIH = superoinferior height of the femoral head; SIN = superoinferior height of the femoral neck; SD = standard deviation; TotW = total mediolateral width of the proximal femur.

SOM Table S2

Summary of the main femoral traits qualitatively described in this study and compared with previously published reports.

		Rose et al., 1996	Nakatsukasa et al., 1998	Ishida et al., 2004	Nakatsukasa et al., 2012	Kikuchi et al., 2018	This study[a]
Proximal	FH				Strong anteversion; weak anterior displacement of the FH center related to FN axis	Inclined weakly anteriorly; rounded	Absence of strong anteversion
	Articular surface FH		Moderately wide	Mediolaterally deep	Extensive and mushrooms over the neck	Moderately wide coverage, mushroomed around the neck	Hemispherical
	FH-GT projection			FH slightly above GT	FH slightly above GT	FH higher than GT	FH above GT
	FH/FN relation				Large	Large (FN constricted superoinferiorly relative to the FH)	Small relative FH
	Fovea capitis				Antero-posteriorly oblong, posteroinferiorly situated	Faint, positioned posteroinferiorly	Shallow; positioned in the distal half of the FH
	FN length			Relatively short	Apparently short	Relatively short	Moderately long
	NSangle		High	High	High		Moderately high
	Lateral flare GT	Protuberant	Flare of the m gluteus minimus insertion		Protuberant insertion of m gluteus minimus	Projects laterally (mainly the distal part)	Inconclusive

	LT	More lateral than posterior projection	Large	Posteromedially directed	Superoinferiorly wide and projects medially	High position, long, projecting medially and moderately posteriorly	Posteromedial direction, close to the FN
	Gluteal tuberosity	Discrete and protuberant		Prominent	Proximally placed (close to the insertion of the m gluteus minimus)		Marked, close to the GT
Distal	Patellar surface		Wide	Squared-shaped	Squared-shaped and wide		Squared-shaped and shallow
	Epicondyles			Similar mediolateral breath	Symmetrical		Symmetrical

Abbreviations: FH = femoral head; FN = femoral neck; GT = greater trochanter; LT = lesser trochanter; m = muscle; NSangle = neck-shaft angle.

[a]See also Pina et al. (2018).

SOM Table S3

Descriptive statistics for SIH/(√SIN*APN) (upper row), relative NL (middle row), and NSangle (bottom row) for each species in the sample of extant anthropoids.

Species	*n*	Mean	SD	Min	Max
Cebus apella	33	1.55	0.07	1.41	1.70
	27	49.70	3.98	40.70	59.04
	27	121.16	5.40	111.99	133.20
Ateles sp.	8	1.67	0.13	1.51	1.94
	8	48.60	5.50	39.88	56.73
	8	127.60	6.24	118.20	134.15
Aloutta sp.	45	1.70	0.11	1.48	1.97
	28	45.09	4.29	31.14	52.62
	30	123.62	6.02	111.03	134.48
Presbytis sp.	34	1.47	0.06	1.37	1.66
	25	42.48	4.00	34.29	53.36
	33	113.23	4.23	103.77	122.19
Colobus sp.	28	1.44	0.09	1.27	1.63
	32	41.59	5.15	30.45	49.49
	27	112.94	6.24	97.86	126.27
Nasalis larvatus	25	1.43	0.09	1.24	1.57
	25	38.14	4.06	29.24	47.52
	25	111.55	4.71	101.33	120.52
Chlorocebus sp.	16	1.45	0.08	1.32	1.60
	10	40.23	4.19	33.25	46.41
	—	—	—	—	—
Cercopithecus sp.	49	1.46	0.09	1.17	1.70
	37	42.27	5.69	32.00	55.61
	14	112.11	4.89	104.15	123.18
Macaca sp.	30	1.44	0.09	1.31	1.64
	27	38.67	5.07	26.36	46.76
	26	110.53	4.67	101.93	120.16
Lophocebus sp.	15	1.49	0.08	1.37	1.65
	7	39.31	4.07	33.71	45.92
	—	—	—	—	—
Mandrillus sp.	13	1.46	0.11	1.31	1.69å
	10	45.40	6.32	37.39	57.11
	10	109.32	6.26	97.84	117.42
Papio sp.	25	1.57	0.10	1.38	1.78
	18	42.91	4.71	35.77	53.70
	20	112.70	5.65	100.18	119.31
Hylobates lar	26	1.89	0.14	1.65	2.12
	25	35.08	3.65	28.33	42.19

	26	123.95	5.16	115.43	134.82
Pongo pygmaeus	12	1.93	0.14	1.70	2.14
	11	48.84	5.83	38.10	54.69
	12	134.93	5.81	127.29	145.07
Pan t. troglodytes	29	1.63	0.08	1.46	1.78
	17	44.47	5.67	36.73	52.97
	—	—	—	—	—
Pan t. schweinfurthii	25	1.68	0.10	1.53	1.94
	21	42.98	5.34	30.50	53.24
	26	123.00	5.11	114.27	132.69
Pan paniscus	20	1.66	0.10	1.53	1.84
	20	38.44	4.65	28.82	44.80
	20	122.77	5.31	114.23	130.86
Gorilla g. gorilla	31	1.65	0.09	1.48	1.81
	20	44.87	5.00	34.08	56.63
	26	121.95	3.98	113.31	127.82
Gorilla b. graueri	21	1.66	0.08	1.49	1.87
	22	42.49	3.75	34.31	50.51
	20	116.89	4.27	107.75	122.61
Gorilla b. beringei	10	1.60	0.07	1.47	1.77
	7	42.00	4.05	33.22	44.79
	9	120.96	4.92	113.94	129.04

Abbreviations: APN = anteroposterior neck depth; *n* = sample size; Max = maximum value; Min = minimum value; NL = neck length; NSangle = neck-shaft angle; SIH = superoinferior height of the femoral head; SIN = superoinferior height of the femoral neck; SD = standard deviation.

SOM References

Ishida, H., Kuminatsu, Y., Takano, T., Nakano, Y., Nakatsukasa, M., 2004. *Nacholapithecus* skeleton from the Middle Miocene of Kenya. J. Hum. Evol. 46, 69-103.

Kikuchi, Y., Nakatsukasa, M., Tsujikawa, H., Nakano, Y., Kunimatsu, Y., Ogihara, N., Shimizu, D., Takano, T., Nakaya, H., Sawada, Y., Ishida, H., 2018. Sexual dimorphism of body size in an African fossil ape, *Nacholapithecus kerioi*. J. Hum. Evol. 123, 129-140.

Nakatsukasa, M., Yamanaka, A., Kunimatsu, Y., Shimizu, D., Ishida, H., 1998. A newly discovered *Kenyapithecus* skeleton and its implications for the evolution of positional behavior in Miocene East African hominoids. J. Hum. Evol. 34, 657-664.

Nakatsukasa, M., Kunimatsu, Y., Shimizu, D., Nakano, Y., Kikuchi, Y., Ishida, H., 2012. Hind limb of the *Nacholapithecus kerioi* holotype and implications for its positional behavior. Anthropol. Sci. 120, 235-250.

Pina, M., Kikuchi, Y., Nakatsukasa, M., Nakano, Y., Kunimatsu, Y., Ogihara, N., Shimizu, D., Takano, T., Tsujikawa, H., Ishida, H., 2018. Revisiting the femoral morphology of *Nacholapithecus kerioi*. Anthropol. Sci. 126, 188.

Rose, M.D., Nakano, Y., Ishida, H., 1996. *Kenyapithecus* postcranial specimens from Nachola, Kenya. Afr. Study Monogr. Suppl. 24, 3-56.